Geomechanics and Engineering, *Vol. 39, No. 1 (2024) 55-72*
https://doi.org/10.12989/gae.2024.39.1.055

Dynamic analysis of viscoelastic FGM shells with porosities on elastic foundation

Mehmet Halil Çalım[1], Ömer Faruk Çapar[2], Mehmet Buğra Özbey[2] and Yavuz Cetin Cuma*[2]

[1]*Department of Civil Engineering, Çukurova University, Adana, Türkiye*
[2]*Department of Civil Engineering, Adana Alparslan Turkes Science and Technology University, Türkiye*

(*Received March 10, 2023, Revised September 6, 2024, Accepted September 9, 2024*)

Abstract. This study investigates free and damped vibration behaviours of porous functionally graded shells supported by Winkler-Pasternak foundation, considering different geometries. Utilizing a higher-order shear deformation theory, the displacement field is determined. The equations of motion are formulated using Hamilton's principle, and the solutions are obtained Navier's method employing double Fourier series. Parametric studies regarding the effects of porosity, material distribution, elastic foundation, shell geometry and damping are carried out. Results are given in tabular and graphical form for the free and forced vibration analyses, respectively.

Keywords: elastic foundation, free vibration, forced vibration, functionally graded materials; porosity; viscoelasticity

1. Introduction

A soil's fines content greatly influences its mechanics and geotechnical engineering (Shariati *et al*. 2019, 2020, Dai *et al*. 2019, Jin *et al*. 2021a). When a constant sub-zero temperature is applied to the surface of a fine-grained soil, a frost front (the 0°C isotherm) progresses through it. Frost heave initiates through not only the in situ freezing of pore water, but also through water entering from unfrozen soil or an external source (Konrad and Morgenstern 1980, Seto and Konrad 1994, Jin *et al*. 2021). In contrast, coarse-grained soils often avoid frost heave, and are usually considered to be non-frost-susceptible. However, the presence of fines in coarse-grained soil affects the soil's frost susceptibility (Konrad and Lemieux 2005).

Frost susceptibility classification criteria are an enduring issue in frozen ground engineering. Over 100 frost susceptibility classification methods have been proposed (Chamberlain 1981, Konrad 1999), and geotechnical engineers have not yet agreed a common standard for cold regions design. Jin *et al*.'s (2017) review of frost susceptibility criteria concluded that criteria derived from laboratory frost heave testing are the most appropriate, being more suitable than other criteria such as particle grading. Since Konrad and Morgenstern's (1980, 1981) innovative accounting of ice segregation in freezing soils and their proposed Segregation Potential (SP), SP has become one of the most widely used indicators for frozen soils obtained from laboratory frost heave testing. Specifically, the SP at the onset of formation of the last ice lens (near the thermal steady-state condition, t_p) in step-freezing tests is a representative value applicable in the field due to the low freezing rate (Konrad 1994, 1988, 1989a, 1999, 2005, Saarelainen 1996, Dore *et al*. 2006). Despite the excellent field reproducibility and applicability of the SP at the onset of formation of the last ice lens, the determination process requires extremely specialized and complicated skills. That is, foundation engineering design in cold regions requires a simple analysis method for engineering application since the specialized and complicated skills are needed for direct classification using the representative SP (Konrad 1999).

Jin *et al*. (2021) proposed a simple method to derive the representative SP, involving empirical semi-log fitting combined with simple laboratory frost heave testing using a temperature-controllable cell. The newly proposed SP determination method was cross-checked using frost ratio (F_z) concept which is newly defined by calculating the ratio of the area of the normalized triangle consisting of the initial and final linear temperature line and the area of the temperature profile at a certain. However, the reported application and verification only considered fine-grained soils. Tester and Gaskin (1996) conducted frost heave test considering fines contents ranging from 2% to 14% weight fraction using the CRREL II (Cold Regions Research and Engineering Laboratory) frost heave testing method and frost susceptibility classification criterion (Chamberlain, 1987). Based on the CRREL II criterion using heave rate, not the representative SP, frost susceptibility increased as fines content increased. Konrad and Lemieux (2005) also analyzed the correlation between the representative SP and fines content, but did not analyze frost susceptibility classification.

This paper reports experimental research to supplement limited data considering frost susceptibility classification using the representative SP as well as frost heave behavior with respect to fines content. Empirical semi-log fitting was also applied to soil mixtures containing various fines contents. In discussion part, the threshold of fines contents

*Corresponding author, Ph.D.
E-mail: cumayc@atu.edu.tr

ISSN: 2005-307X (Print), 2092-6219 (Online)

as well as the reliability of the empirical semi-log fitting were assessed in detail using the representative S Shells of numerous geometrical shapes are essential structural element in numerous engineering fields, including automobile bodies, slabs, panels, spaceship tiles. It can be easily understood that shell structures are under continuous dynamic loading. Therefore, studying the dynamic response of shells is crucial. In order to present the dynamic nature of these structural components many studies are published and available in the literature. A survey about the shells regarding various analysis methods, shell geometries, materials, shell theories, shear deformation theories and boundary conditions is carried out. A summary of the encountered papers is given with their respective references.

Sofiyev (2010) conducted a buckling analysis of simply supported truncated conical shells made from functionally graded materials (FGMs), focusing on the impact of axial compressive loads and elastic foundations. The study utilized modified Donnell-type equations solved with Galerkin's method to determine critical loads and examined the influences of various material distributions and foundation models on the buckling responses of FGM shells. Duc and Quan (2014) investigated the dynamic analysis of FG double-curved thin shallow shells supported by elastic foundation, investigating the impacts of various foundation properties, porosity, and temperature.

Kim (2015) and Li *et al.* (2019 a, b) determined the displacement fields utilizing first order shear deformation theory (FSDT) and solved the differential equations for FG shell using Rayleigh-Ritz method to obtain the fundamental frequencies of FG cylindrical shell. Quan and Duc (2016) conducted a dynamic analysis of imperfect functionally graded materials (FGM) thick double-curved shallow shells supported by elastic foundations, incorporating material properties that vary with thickness, power law index, and temperature. Their analysis examined the effects of various geometric and material properties, temperature, and the elastic foundation on the results. Wang and Wu (2017) obtained the displacement field of PFG cylindrical shell by using SSDT and solved equations of motion by applying Rayleigh-Ritz method in free vibration analysis. Their investigation regards the influence of boundary conditions, geometric properties and porosity distribution on the analysis. Younsi *et al.* (2018) performed bending and free vibration analyses of functionally graded (FG) plates utilizing theories that involve more complex integrals and fewer unknowns compared to higher-order shear deformation theories (HSDT). Their analysis utilized material properties that vary according to power-law, exponential, and Mori-Tanaka models. Zouatnia *et al.* (2018) introduced a refined shear deformation theory for analysing the free vibration of functionally graded plates under various boundary conditions. Their theory, which simplifies the number of unknowns and eliminates the need for shear correction factors, is compared with other shear deformation theories through numerical results that assess the influences of boundary conditions, power-law index, aspect ratio, and side-to-thickness ratio. Mehala *et al.* (2018) investigated the effects of different homogenization models on the buckling and free vibration of functionally graded plates (FGMs) supported by elastic foundations and compared their analytical results with predictions from other plate theories. Bayat *et al.* (2018) explored the nonlinear vibrations of Euler-Bernoulli beams on a linear elastic foundation, offering a semi-analytical solution with high accuracy. They analysed conducted the analytical solution using Runge-Kutta method to observe the impacts of the foundation and various parameters on the linear frequencies. Barati and Zenkour (2019) obtained the displacement fields utilizing FSDT and conducted the analytical solution using Galerkin method. They investigated the variation fundamental frequencies of porous nanocomposite shell reinforced with graphene platelets, considering the effects of graphene platelet reinforcement, foundation parameters, and various porosity characteristics. Liang *et al.* (2019) performed a free vibration analysis of FG cylindrical shell by comparing a semi analytical method, determined by combining the differential quadrature method with Durbin's modified inverse Laplace transform, with the Navier analytical solution method. Zhao *et al.* (2019) examined the vibration characteristics of functionally graded porous shallow shells with general boundary conditions. They used a simplified virtual spring technique for boundary conditions and a modified Fourier series to accurately compute natural frequencies and mode shapes. Sobhy and Zenkour (2019) analysed the fundamental frequencies of functionally graded graphene platelet-reinforced composite doubly-curved shells using a four-variable shear deformation theory. Their study examined the impacts of various boundary conditions, graphene distribution, and shell curvature on these frequencies. Ahmadi (2019) explored a nonlinear elastic foundation model with three parameters.

They utilized Galerkin method to derive an analytical solution and investigated the primary resonance behaviour of cylindrical shell. Ahmadi and Foroutan (2019) investigated the impacts of thermal environment, elastic foundation support, and stiffeners on the resonances of functionally graded (FG) cylindrical shell. Merzoug *et al.* (2020) performed bending analysis on functionally graded (FG) beams supported by two-layer elastic foundations under thermos-mechanical loads, examining the influences of various micromechanical and foundation parameters, as well as geometric and temperature characteristics. Foroutan and Ahmadi (2020) investigated the impacts of porosity distributions, material properties, and elastic foundation support on the buckling response of FG porous cylindrical shell using the fourth order Runge-Kutta method. Faleh *et al.* (2020) used strain gradient theory and FSDT to perform forced vibration on porous crystal nano shells subjected to impact loads. Nebab *et al.* (2020) performed a dynamic analysis of advanced composite plates supported by variable elastic foundations, considering material properties that vary with thickness and power law coefficients. They employed a higher-order shear deformation theory (HSDT) and the Mori-Tanaka model to derive displacement fields. The differential equations were formulated utilizing Hamilton's principle and solved with the Navier method.

The study investigated the impact of three different distributions of the Pasternak foundation parameter and

variable material properties on the dynamic response of advanced composite plates supported by variable elastic foundations. Ahmadi and Foroutan (2020) conducted a thermal buckling analysis of FG multilayered cylindrical shell with porous core, using semi-analytical and analytical methods. They employed Runge-Kutta method to determine the thermal buckling results. Rahimi *et al.* (2020) examined the bending and free vibration behaviour of functionally graded graphene platelet–reinforced composite porous cylindrical shells using elasticity theory. They applied analytical and numerical methods to study the effects of graphene distribution, porosity patterns, and shell geometry on its mechanical behaviour. Rabhi *et al.* (2020) performed buckling and vibration analyses of exponentially graded sandwich plates resting on elastic mediums under various boundary conditions, utilizing their proposed trigonometric shear deformation theory with three unknowns. Salehipour *et al.* (2020) explored the bending and free vibration behaviours of porous and functionally graded cylindrical micro/nano shells using modified couple stress and three-dimensional elasticity theories. Their study employed Hamilton's principle and the generalized differential quadrature method to analyse the impacts of material property gradients, porosity, and length scale parameters. Rachedi *et al.* (2020) explored the thermo-mechanical bending of functionally graded plates on variable elastic foundations utilizing a quasi-3D shear deformation theory. They derived the equations of motion with various homogenization models and validated the accuracy and simplicity of their approach by obtaining deflections and stresses under temperature-dependent conditions. Qin *et al.* (2020) conducted a free vibration analysis of thick functionally graded porous graphene platelet reinforced composite cylindrical shells, examining the effects of various foundation models, boundary conditions, porosity distributions, and graphene platelet distributions. Chikr *et al.* (2020) utilized FSDT and Galerkin method to study the influences of various boundary conditions, geometric and foundation properties on the buckling response of sandwich plates on an elastic foundation. Sea-Long *et al.* (2021) proposed a flexibility-based beam-foundation model for analysing both elastic and inelastic beam-foundation systems, using the Winkler-Pasternak foundation. Fu *et al.* (2021a, b) performed vibration analyses for conical shells using FSDT and examined the effects of various parameters. Cuong-Le *et al.* (2021) conducted free and buckling analyses of shell, focusing on the impacts of different shell geometries and the use of porous rock materials. Zhang *et al.* (2021) examined the vibrational behaviour of a three-layered cylindrical shell with a functionally graded porous core and nanocomposite face sheets supported by a Pasternak foundation. They analysed how the dispersion pattern of graphene nanoplatelets and *al.* (2022) investigated the impacts of different porosity distributions, foundation coefficients and properties of the porous core on the natural frequencies of FG sandwich beams with porous core supported by elastic foundation. The displacement fields were derived employing trigonometric shear deformation theories, and the equations of motion were formulated through Hamilton's principle. Said (2023) investigated wave propagation in a nonlocal porous thermoelastic half-space with temperature-dependent properties using Green-Lindsay and Lord-Shulman theories. The study solves the governing equations through normal mode analysis and explores the effects of temperature variations. Alimoradzadeh and Akbaş (2023) applied Galerkin method to solve the equations of motion derived utilizing Hamilton's principle. They observed the effects of viscoelastic foundation and various distribution of carbon nanotube reinforcement on the free vibration analysis of composite beam. Bennedjadi *et al.* (2023) derived the equations of motion using virtual work method and solved them using Galerkin method. They examined the impacts of various boundary conditions, foundation properties, and damping coefficients on the buckling response of an exponentially graded sandwich plate. Limkatanyu *et al.* (2023) introduced a new frame element for analysing non-ductile reinforced concrete members on a Winkler-Pasternak foundation, incorporating shear-flexure interactions. Their formulation is based on Timoshenko beam theory. Sobhani *et al.* (2023) combine FSDT with Donnell's shell theory to develop the formulation and use the Generalized Differential Quadrature Method for analytical solutions. They investigate the impact of boundary conditions and types of elastic foundations on the natural frequencies of Graphene Oxide Powder (GOP) nanocomposite cylindrical shells. He *et al.* (2023) used FSDT, Hamilton principle, and Runge-Kutta method to perform vibration analysis of laminated carbon fiber reinforced resin doubly hallow shell with a porous microcapsule coating. They investigated the impacts of temperature, humidity, geometric parameters, and porosity on the shell's vibration response. Khaniki and Ghayesh (2023) explored the effects of different shell geometries on free and forced vibration analysis of shell by employing Donnell's nonlinear shell theory, Mooney-Rivlin strain energy density model, Hamilton's principle, Galerkin method, and Newton-Raphson approach.

Liu *et al.* (2022) investigated the structural response of U-type corrugated core sandwich panels under lateral quasi-static compression. Gao *et al.* (2022) use a multi-step approach to predict the in plane elastic properties of structures with negative Poisson's ratio. Zhang and Zhang (2023) used viscoelastic materials to mitigate earthquake-induced pounding in soil-structure intersections. Cheng *et al.* (2024) investigated the effects of temperature and porosity on the seismic responses of geothermal reservoirs. Wu *et al.* (2024) studied the exact expressions for the scattering of various plane waves in an infinite periodic array for the application in engineering structures. Zhang *et al.* (2024) developed an active vibration control method in order to supress the vibrations of a ship pipeline.

Following a thorough search in the literature, it is understood that, although there are many papers considering shells with porous functionally graded (PFG) materials supported by elastic foundation there is still a lack regarding the forced vibration analysis on the matter using viscoelastic material model. In fact, as far as Authors' knowledge, this study is the first report on the damped forced vibration analysis of PFG viscoelastic shells resting

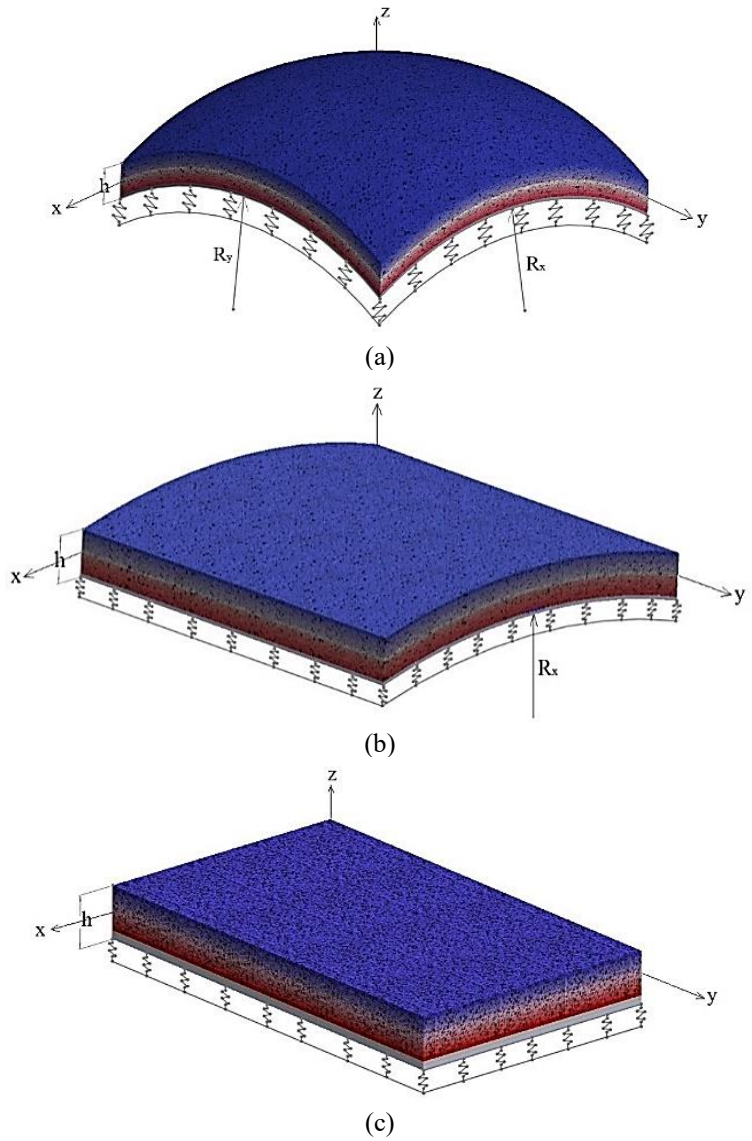

Fig. 1 (a) Spherical shell, (b) cylindrical shell and (c) plate resting on elastic foundation

on elastic foundation. The material properties are incorporated into the analyses using one of the most popular viscoelastic models (Kelvin viscoelastic model). The displacement field of the shells are obtained through a HSDT. By implementing Hamilton's principle, the equations of motion are derived in Laplace domain including the foundation parameters. The system equations are solved utilizing Navier's method, and the results are then converted back to the time domain employing Durbin's modified inverse Laplace transform algorithm (Calim 2003, Calim 2016;, Calim and Cuma 2022, 2023).

Various mechanical properties are investigated in the present study. The effect of shell geometry is studied by regarding spherical, cylindrical and plate type geometries. Also, influence of the foundation on the shell is investigated by using Winkler-Pasternak foundation model. Furthermore, the impact of material properties is presented by considering viscoelasticity, porosity and the rate of material distribution. Viscoelasticity of the material is modelled with Kelvin's viscoelastic material model. Porosity of the material composition is considered to be evenly distributed. Also, rate of change of the material is expressed with the power law distribution. Verification of the proposed model is accomplished by comparing the obtained free vibration analysis results with the ones available in the literature. Subsequently, a parametric free vibration analysis is completed, and its results are given in tabulated form. Finally, a parametric damped forced vibration analyses are performed considering all aforementioned properties and the results are presented by graphical form in contrast of various parameters.

2. Formulation

FGM porous shells shown in Figs. 1(a)-1(c) have length of a, width of b and thickness of h. The radii of curvature in the x and y directions, denoted as R_x and R_y respectively, define the geometric shape of the porous FGM shell. By changing these radii, different geometrical shapes can be

achieved: a plate is obtained when $R_x = R_y = \infty$, a spherical shell when $R_x = R_y \neq \infty$, and a cylindrical shell when $R_y = \infty$ and $R_x \neq \infty$. The FGM porous shells in Figs. 1(a)-1(c) are supported by elastic foundation.

The materials of the shell structures are distributed via the well-known power law. The mechanical properties of the materials (Young's modulus (E), mass density (ρ), Poisson's ratio (v) and shear modulus (G)) change through the thickness of the shell via a function of z (Jouneghani *et al.* 2017, Wang *et al.* 2018, Trinh and Kim 2019, Fu *et al.* 2020, Salehipour *et al.* 2020, Tran *et al.* 2021, Sharma *et al.* 2021, Timesli 2022, Swaminathan *et al.* 2022).

$$P(z) = P_m + (P_c - P_m)\left(0.5 + {}^{z}/_{h}\right)^{p_l} - {}^{p_r}/_{2}\,(P_c + P_m) \tag{1}$$

where P_m denotes metal properties, P_c denotes ceramic properties, p_l denotes power law coefficient and p_r denotes porosity coefficient.

In order to obtain more accurate results as the material properties are changing throughout the thickness, complex shear deformation functions are to be used. Using HSDT, displacement fields are obtained as follows.

$$\begin{Bmatrix} u(x,y,z,t) \\ v(x,y,z,t) \\ w(x,y,z,t) \end{Bmatrix} = \begin{Bmatrix} \left(1+\frac{z}{R_x}\right)u_o \\ \left(1+\frac{z}{R_y}\right)v_o \\ w_o \end{Bmatrix} - z\begin{Bmatrix} w_{o,x} \\ w_{o,y} \\ 0 \end{Bmatrix} + f(z)\begin{Bmatrix} \theta \\ \psi \\ 0 \end{Bmatrix} \tag{2}$$

Central displacements of shells in the x, y and z directions are denoted as u_o, v_o and w_o, respectively. θ and ψ are rotations of section normal. Additionally, $(\,)_{,x}$ and $(\,)_{,y}$ are partial derivatives with respect to x and y, respectively. $f(z)$ in Eq. (2) represents the shape function of the HSDT and is given in Eq. (3) which has been used by various researchers (Rachid *et al*. 2022, Zaoui *et al*. 2019).

$$f(z) = \frac{\pi\, h}{\pi^4 + h^4} e^{\left(\frac{hz}{\pi}\right)}\left(\pi^2 sin\left(\frac{\pi z}{h}\right) + h^2 cos\left(\frac{\pi z}{h}\right)\right) - \frac{\pi\, h^3}{\pi^4 + h^4} \tag{3}$$

With the help of linear elasticity theory, the connection between displacement and normal-shear strains can be established as follows.

$$\begin{aligned} \varepsilon_x &= \frac{\partial u}{\partial x} + \frac{w_0}{R_x} \\ \varepsilon_y &= \frac{\partial v}{\partial y} + \frac{w_0}{R_y} \\ \gamma_{yz} &= \frac{\partial v}{\partial z} + \frac{\partial w}{\partial y} - \frac{v_0}{R_y} \\ \gamma_{xz} &= \frac{\partial u}{\partial z} + \frac{\partial w}{\partial x} - \frac{u_0}{R_x} \\ \gamma_{xy} &= \frac{\partial u}{\partial y} + \frac{\partial v}{\partial x} \end{aligned} \tag{4}$$

Eq. (4) can be transformed into matrix form as can be seen in Eq. (5) (Sayyad and Ghugal 2019, 2022, Vinh and Tounsi 2022, Malaibari *et al*. 2022)

$$\begin{bmatrix} \varepsilon_x \\ \varepsilon_y \\ \gamma_{yz} \\ \gamma_{xz} \\ \gamma_{xy} \end{bmatrix} = \begin{bmatrix} \frac{\partial}{\partial x} & 0 & \frac{1}{R_x} - z\frac{\partial^2}{\partial x^2} & f(z)\frac{\partial}{\partial x} & 0 \\ 0 & \frac{\partial}{\partial y} & \frac{1}{R_y} - z\frac{\partial^2}{\partial y^2} & 0 & f(z)\frac{\partial}{\partial y} \\ 0 & 0 & 0 & f'(z) & 0 \\ 0 & 0 & 0 & 0 & f'(z) \\ \frac{\partial}{\partial y} & \frac{\partial}{\partial x} & -2z\frac{\partial}{\partial x}\frac{\partial}{\partial y} & f(z)\frac{\partial}{\partial y} & f(z)\frac{\partial}{\partial x} \end{bmatrix} \begin{bmatrix} u_o \\ v_o \\ w_o \\ \theta \\ \psi \end{bmatrix} \tag{5}$$

Considering the thickness of FGM porous shell is rather small compared to the displacements, σ_z and ε_z may be taken as zero. The stress-strain relation for the FGM porous shell is as follows.

$$\begin{aligned} \sigma_x &= C_{11}\varepsilon_x + C_{12}\varepsilon_y \\ \sigma_y &= C_{21}\varepsilon_x + C_{22}\varepsilon_y \\ \tau_{yz} &= C_{44}\gamma_{yz} \\ \tau_{xz} &= C_{55}\gamma_{xz} \\ \tau_{xy} &= C_{66}\gamma_{xy} \end{aligned} \tag{6}$$

where the coefficients C represent the stiffness parameters which can be obtained as follows.

$$\begin{aligned} C_{11} = C_{22} &= \frac{E(z)}{(1-\nu^2)} \\ C_{12} = C_{21} &= \frac{\nu E(z)}{(1-\nu^2)} \\ C_{44} = C_{55} = C_{66} &= \frac{E(z)}{2(1+\nu)} \end{aligned} \tag{7}$$

The variation of strain energy caused by elastic deformation is defined as follows.

$$\delta U = \int_A \int_{-h/2}^{h/2} \left(\sigma_x \delta\varepsilon_x + \sigma_y\, \delta\varepsilon_y + \tau_{xy}\delta\gamma_{xy} + \tau_{xz}\delta\gamma_{xz} + \tau_{yz}\delta\gamma_{yz}\right) dz\, dA \tag{8}$$

The change of kinetic energy can be determined as shown in Eq. (9).

$$\delta T = \int_A \int_{-h/2}^{h/2} \rho(z)(-\ddot{u}\delta u - \ddot{v}\delta v - \ddot{w}\delta w)\, dz\, dA \tag{9}$$

here $(\dot{\ })$ represents partial derivative with respect to t and $\rho(z)$ denotes mass density as a function of thickness. V represents potential energy and the variation of V can be determined as below.

$$\delta V = \int_A q(x,y)\, \delta w\, dA \tag{10}$$

The energy resulting from the elastic foundation is denoted by V_e and can be expressed as follows.

$$\delta V = \int_A q(x,y)\, \delta w\, dA \tag{11}$$

The equations of motion for FGM porous shell can be derived utilizing Hamilton's principle as outlined below.

$$\int_{t_1}^{t_2} (\delta U - \delta T - \delta V + \delta V_e) dt = 0 \tag{12}$$

Relations of Stress-strain in Eq. (6) and strain-displacement in Eq. (5) are used to obtained forces and moment.

$$\{N_x, N_y, N_{xy}\} = \int_{-\frac{h}{2}}^{\frac{h}{2}} \{\sigma_x, \sigma_y, \tau_{xy}\}\, dz \tag{13}$$

$$\{Q_x, Q_y\} = \int_{-h/2}^{h/2} \{\tau_{xz}, \tau_{yz}\} f'(z)\, dz$$

$$\{M_x^b, M_y^b, M_{xy}^b\} = \int_{-\frac{h}{2}}^{\frac{h}{2}} \{\sigma_x, \sigma_y, \tau_{xy}\}\, z\, dz$$

$$\{M_x^s, M_y^s, M_{xy}^s\} = \int_{-h/2}^{h/2} \{\sigma_x, \sigma_y, \tau_{xy}\}\, f(z)\, dz$$

I represent inertia components and is defined as follows.

$$\{I_1, I_2, I_3, I_4, I_5, I_6\} = \int_{-h/2}^{h/2} \rho(z)\{1, z, z^2, f(z), zf(z), f(z)^2\}\, dz \tag{14}$$

By substituting Eqs. (8)-(11) into Eq. (12) and applying Eqs. (13) and (14), the following expression can be obtained.

$$\begin{gathered}
-N_{x,x}\delta u_0 + \tfrac{N_x}{R_x}\delta w_0 - M_{x,xx}^b \delta w_0 - M_{x,x}^s \delta\theta_0 - \\
N_{y,y}\delta v_0 + \tfrac{N_y}{R_y}\delta w_0 - M_{y,yy}^b \delta w_0 - M_{y,y}^s \delta\psi_0 - \\
N_{xy,y}\delta u_0 - N_{xy,x}\delta v_0 - 2M_{xy,xy}^b \delta w_0 - M_{xy,y}^s \delta\theta_0 - \\
M_{xy,x}^s \delta\psi_0 + Q_x\,\delta\theta_0 + Q_y\delta\psi_0 + I_1 \ddot{u}_o \delta u_0 + \\
2\,\tfrac{I_2\,\ddot{u}_o}{R_x}\delta u_0 + I_2\,\ddot{u}_{o,x}\delta w_0 + I_4\,\ddot{u}_o\delta\theta_0 + \tfrac{I_3\,\ddot{u}_o}{{R_x}^2}\delta u_0 + \\
\tfrac{I_3\,\ddot{u}_{o,x}}{R_x}\delta w_0 + \tfrac{I_5\,\ddot{u}_o}{R_x}\delta\theta_0 - I_2\,\ddot{w}_{0,x}\delta u_0 - \tfrac{I_3\,\ddot{w}_{0,x}}{R_x}\delta u_0 - \\
I_3\,\ddot{w}_{0,xx}\delta w_0 - I_5\,\ddot{w}_{0,x}\delta\theta_0 + I_4\,\ddot{\theta}_0\,\delta u_0 + \rho(z)\tfrac{I_5\,\ddot{\theta}_0}{R_x}\delta u_0 + \\
I_5\,\ddot{\theta}_{0,x}\delta w_0 + I_6\,\ddot{\theta}_0\,\delta\theta_0 + I_1\ddot{v}_o\delta v_0 + 2\,\tfrac{I_2\,\ddot{v}_o}{R_y}\delta v_0 + \\
I_2\,\ddot{v}_{o,y}\delta w_0 + I_4\,\ddot{v}_o\delta\psi_0 + \tfrac{I_3\,\ddot{v}_o}{{R_y}^2}\delta v_0 + \tfrac{I_3\,\ddot{v}_{o,y}}{R_y}\delta w_0 + \\
\tfrac{I_5\,\ddot{v}_o}{R_y}\delta\psi_0 - I_2\,\ddot{w}_{0,y}\delta v_0 - \tfrac{I_3\,\ddot{w}_{0,y}}{R_x}\delta v_0 - I_3\,\ddot{w}_{0,yy}\delta w_0 - \\
I_5\,\ddot{w}_{0,y}\delta\psi_0 + I_4\,\ddot{\psi}_0\delta v_0 + \tfrac{I_5\,\ddot{\psi}_0}{R_y}\delta v_0 + I_5\,\ddot{\psi}_{0,y}w_0 + \\
I_6\,\ddot{\psi}_0\delta\psi_0 + I_1\ddot{w}_0\delta w_0 - q(x,y)\,\delta w_0 + k_0 w_0\delta w_0 - \\
k_1 w_{0,xx}\delta w_0 - k_1 w_{0,yy}\delta w_0 = 0
\end{gathered} \tag{15}$$

By grouping the terms in Eq. (15) under the coefficients of δu_0, δv_0, δw_0, $\delta\theta_0$, $\delta\psi_0$ the following expressions can be obtained.

$$\begin{gathered}
-N_{x,x} - N_{xy,y} + I_1\ddot{u}_o + 2\,I_2\tfrac{\ddot{u}_o}{R_x} + I_3\tfrac{\ddot{u}_o}{{R_x}^2} - I_2\ddot{w}_{o,x} - I_3\tfrac{\ddot{w}_{o,x}}{R_x} + \\
I_4\ddot{\theta}_0 + I_5\tfrac{\ddot{\theta}_0}{R_x} = 0
\end{gathered}$$

$$\begin{gathered}
-N_{y,y} - N_{xy,x} + I_1\ddot{v}_o + 2\,I_2\frac{\ddot{v}_o}{R_y} + I_3\frac{\ddot{v}_o}{{R_y}^2} - I_2\ddot{w}_{o,y} - I_3\frac{\ddot{w}_{o,y}}{R_y} \\
+ I_4\ddot{\psi}_0 + I_5\frac{\ddot{\psi}_0}{R_y} = 0
\end{gathered}$$

$$\begin{gathered}
-M_{x,xx}^b - M_{y,yy}^b - 2M_{xy,xy}^b + \frac{N_x}{R_x} + \frac{N_y}{R_y} + I_1\ddot{w}_o \\
+ I_2\big(\ddot{u}_{o,x} + \ddot{v}_{o,y}\big) - I_3\big(\ddot{w}_{o,xx} + \ddot{w}_{o,yy}\big) \\
+ \frac{I_3\ddot{u}_{o,x}}{R_x} + \frac{I_3\ddot{v}_{o,y}}{R_y} + I_5\big(\ddot{\theta}_{0,x} + \ddot{\psi}_{0,y}\big) \\
- q(x,y) + k_0 w_0 - k_1 w_{0,xx} - k_1 w_{0,yy} \\
= 0
\end{gathered} \tag{16}$$

$$-M_{x,x}^s - M_{xy,y}^s + Q_x + I_4\ddot{u}_o + I_5\tfrac{\ddot{u}_o}{R_x} - I_5\ddot{w}_{o,x} + I_6\ddot{\theta}_o = 0$$

$$-M_{y,y}^s - M_{xy,x}^s + Q_y + I_4\ddot{v}_o + I_5\frac{\ddot{v}_o}{\mathrm{R}_y} - I_5\ddot{w}_{o,y} + I_6\ddot{\psi}_0 = 0$$

Expressions for the moments and forces in Eq. 13 can be obtained with the help of Eqs. (4) and (5).

$$\begin{gathered}
N_x = A_{11}\left(u_{o,x} + \frac{w_0}{R_x}\right) + A_{12}\left(v_{o,y} + \frac{w_0}{R_y}\right) - B_{11}w_{o,xx} - B_{12}w_{o,yy} + A_{s11}\theta_{,x} \\
+ A_{s12}\psi_{,y}
\end{gathered}$$

$$\begin{gathered}
N_y = A_{21}(u_{o,x} + \frac{w_0}{R_x}) + A_{22}(v_{o,y} + \frac{w_0}{R_y}) - B_{21}w_{o,xx} - B_{22}w_{o,yy} + A_{s21}\theta_{,x} \\
+ A_{s22}\psi_{,y}
\end{gathered}$$

$$N_{xy} = A_{66}u_{o,y} + A_{66}v_{o,x} - 2B_{66}w_{o,xy} + A_{s66}\theta_{,y} + A_{s66}\psi_{,x}$$

$$Q_x = A_{cc55}\,\theta$$

$$Q_y = A_{cc44}\,\psi$$

$$\begin{gathered}
M_x^b = B_{11}\left(u_{o,x} + \frac{w_0}{R_x}\right) + B_{12}\left(v_{o,y} + \frac{w_0}{R_y}\right) - D_{11}w_{o,xx} - D_{12}w_{o,yy} + B_{s11}\theta_{,x} \\
+ B_{s12}\psi_{,y}
\end{gathered} \tag{17}$$

$$\begin{gathered}
M_y^b = B_{21}\left(u_{o,x} + \frac{w_0}{R_x}\right) + B_{22}\left(v_{o,y} + \frac{w_0}{R_y}\right) - D_{21}w_{o,xx} - D_{22}w_{o,yy} + B_{s21}\theta_{,x} \\
+ B_{s22}\psi_{,y}
\end{gathered}$$

$$M_{xy}^b = B_{66}u_{o,y} + B_{66}v_{o,x} - 2D_{66}w_{o,xy} + B_{s66}\theta_{,y} + B_{s66}\psi_{,x}$$

$$\begin{gathered}
M_x^s = A_{s11}\left(u_{o,x} + \frac{w_0}{R_x}\right) + A_{s12}\left(v_{o,y} + \frac{w_0}{R_y}\right) - B_{s11}w_{o,xx} - B_{s12}w_{o,yy} \\
+ A_{ss11}\theta_{,x} + A_{ss12}\psi_{,y}
\end{gathered}$$

$$\begin{gathered}
M_y^s = A_{s21}\left(u_{o,x} + \frac{w_0}{R_x}\right) + A_{s22}\left(v_{o,y} + \frac{w_0}{R_y}\right) - B_{s21}w_{o,xx} - B_{s22}w_{o,yy} \\
+ A_{ss21}\theta_{,x} + A_{ss22}\psi_{,y}
\end{gathered}$$

$$M_{xy}^b = A_{s66}u_{o,y} + A_{s66}v_{o,x} - 2B_{s66}w_{o,xy} + A_{ss66}\theta_{,y} + A_{ss66}\psi_{,x}$$

Stiffness components $(A_{ij}, B_{ij}, A_{sij}, D_{ij}, B_{sij}, A_{ccij}, A_{ssij})$ in Eq. (15) can be expressed as below.

$$\begin{gathered}
\{A_{ij}, B_{ij}, A_{sij}, D_{ij}, B_{sij}, A_{ccij}, A_{ssij}\} = \\
\int_{-h/2}^{h/2}\{1, z, f(z), z^2, zf(z), f'(z)^2, f(z)^2\}\, Q_{ij}dz \\
i, j = 1, 2, 6
\end{gathered} \tag{18}$$

For the analytical solution of the equations of motion given in Eq. (16), the displacement components in the Navier's method based on double Fourier series are employed. The displacement components in the Fourier series are as follows.

$$\begin{gathered}
u_o(x,y,t) = \sum_{m=1}^{\infty}\sum_{n=1}^{\infty} U_{mn}\, Cos\left(\frac{m\pi}{a}x\right)\, Sin\left(\frac{n\pi}{b}y\right) Sin(i\omega t) \\
v_o(x,y,t) = \sum_{m=1}^{\infty}\sum_{n=1}^{\infty} V_{mn} Sin\left(\frac{m\pi}{a}x\right) Cos\left(\frac{n\pi}{b}y\right) Sin(i\omega t) \\
w_o(x,y,t) = \sum_{m=1}^{\infty}\sum_{n=1}^{\infty} W_{mn}\, Sin\left(\frac{m\pi}{a}x\right)\, Sin\left(\frac{n\pi}{b}y\right) Sin(i\omega t) \\
\theta(x,y,t) = \sum_{m=1}^{\infty}\sum_{n=1}^{\infty} \theta_{mn}\, Cos\left(\frac{m\pi}{a}x\right)\, Sin\left(\frac{n\pi}{b}y\right) Sin(i\omega t) \\
\psi(x,y,t) = \sum_{m=1}^{\infty}\sum_{n=1}^{\infty} \psi_{mn}\, Sin\left(\frac{m\pi}{a}x\right)\, Cos\left(\frac{n\pi}{b}y\right) Sin(i\omega t)
\end{gathered} \tag{19}$$

Coefficients $(U_{mn}, V_{mn}, W_{mn}, \theta_{mn}, \psi_{mn})$ in Eq. (19) are unknown displacement coefficients and are derived in such a way as to satisfy the specified boundary conditions

outlined below (Reddy 1984, Zenkour *et al.* 2011, Thai and Choi 2011, Tran *et al.* 2017, Kiani *et al.* 2012a, b, Sayyad and Ghugal 2019, 2021, 2022, Nguyen *et al.* 2021, Vu *et al.* 2023).

$$\begin{aligned} u_0(x,0,t) &= u_o(x,b,t) = v_o(0,y,t) = v_o(a,y,t) = 0 \\ w_o(x,0,t) &= w_o(x,b,t) = w_o(0,y,t) = w_o(a,y,t) = 0 \\ M_y^s(x,0,t) &= M_y^s(x,b,t) = M_x^s(0,y,t) = M_x^s(a,y,t) = 0 \\ M_y^b(x,0,t) &= M_y^b(x,b,t) = M_x^b(0,y,t) = M_x^b(a,y,t) = 0 \\ N_y(x,0,t) &= N_y(x,b,t) = N_x(0,y,t) = N_x(a,y,t) = 0 \end{aligned} \tag{20}$$

The distributed dynamic load applied in the gravity direction can be expressed utilizing trigonometric series is as follows.

$$\begin{aligned} q(x,y,t) &= \sum_{m=1}^{\infty}\sum_{n=1}^{\infty} Q_{mn}(t)\ Sin\left(\frac{m\pi x}{a}\right) Sin\left(\frac{n\pi y}{b}\right) \\ Q_{mn}(t) &= \frac{4}{ab}\int_{-a/2}^{a/2}\int_{-b/2}^{b/2} q(x,y,t)\, Sin\left(\frac{m\pi x}{a}\right) Sin\left(\frac{n\pi y}{b}\right) dydx \end{aligned} \tag{21}$$

Laplace transform enables converting a time dependent function to a linear algebraic function. The conversion to Laplace domain discards the necessity of obtaining a proper time step for the analysis allowing the solution to be a simple algebraic solution. Laplace transform of a time-dependent function can be represented as follows.

$$L[f(t)] = \bar{F}(p) = \int_0^{\infty} f(t)\, e^{-pt} dt \tag{22}$$

p is the Laplace transform parameter. First and second derivatives of $f(t)$ over time are given in Laplace domain.

$$\begin{aligned} L\left[\dot{f}(t)\right] &= p\,\bar{F}(p) - f(0) \\ L\left[\ddot{f}(t)\right] &= p^2\bar{F}(p) - pf(0) - \dot{f}(0) \end{aligned} \tag{23}$$

The system is considered stationary at $t = 0$, thus, $\dot{f}(0)$ and $f(0)$ taken zero as initial conditions. The solution of Eq. (24) yields the displacements that must be converted from the Laplace domain to the time domain. Thus, Durbin's modified inverse Laplace transform procedure is employed (For further information please read the following references (Calim 2003, Temel and Calim 2003, Eratli *et al.* 2014, Calim 2016, Türker *et al.* 2023))

The equations of motion in Laplace domain can be expressed in matrix form as follows.

$$\left(\begin{bmatrix} k_{11} & k_{12} & k_{13} & k_{14} & k_{15} \\ . & k_{22} & k_{23} & k_{24} & k_{25} \\ . & . & k_{33} & k_{34} & k_{35} \\ . & . & . & k_{44} & k_{45} \\ . & . & . & . & k_{55} \end{bmatrix} + p^2 \begin{bmatrix} m_{11} & m_{12} & m_{13} & m_{14} & m_{15} \\ . & m_{22} & m_{23} & m_{24} & m_{25} \\ . & . & m_{33} & m_{34} & m_{35} \\ . & . & . & m_{44} & m_{45} \\ . & . & . & . & m_{55} \end{bmatrix}\right) \begin{bmatrix} \bar{U}_{mn} \\ \bar{V}_{mn} \\ \bar{W}_{mn} \\ \bar{\theta}_{mn} \\ \bar{\psi}_{mn} \end{bmatrix} = \begin{bmatrix} \bar{P}_x \\ \bar{P}_y \\ \bar{Q}_{mn} \\ \bar{m}_x \\ \bar{m}_y \end{bmatrix} \tag{24}$$

The closed form of the system matrices can be given as follows.

$$[\boldsymbol{K}_{mn} + p^2\, \boldsymbol{M}_{mn}]\, \bar{\boldsymbol{D}}_{mn} = \bar{\boldsymbol{F}}_{mn} \tag{25}$$

where $\bar{\mathbf{D}}_{mn}$ and $\bar{\mathbf{F}}_{mn}$ represent the unknown displacement vector and the external force vector in Laplace domain,

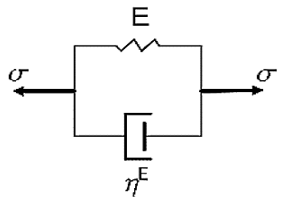

Fig. 2 Kelvin viscoelastic model

respectively. Additionally, **K** and **M** matrices, whose elements are detailed in Appendix A, correspond to the stiffness matrix and the mass matrix, respectively.

The damping effect is included in the forced vibration analysis. Thus, more realistic results are obtained due to material internal friction. One of the two most popular models in the literature many viscoelasticity models is the Kelvin model (Calim 2003, Temel *et al* 2004, Cuma and Calim 2021, 2022).

The elastic constants of Kelvin model can be formulated as shown below by applying the elastic-viscoelastic analogy.

$$\begin{aligned} E_v(z) &= E(z)(1 + g\,p) \\ G_v(z) &= G(z)(1 + g\,p) \end{aligned} \tag{26}$$

Here G_v and E_v represent shear modulus and viscoelastic elasticity. p and g denote the Laplace parameter and damping ratio. By using the correspondence principle viscoelastic material properties are directly used in the algorithm.

3. Numerical examples

Free and forced vibration analyses of FGM porous shells are carried out in this study. Several algorithms are developed by using Mathematica program. Firstly, a comparison study is conducted considering the free vibration analysis of FGM shells supported by elastic foundation. The results produced by the developed algorithm are validated by comparing them with existing data from the literature. Following this, a parametric analysis of the free vibration characteristics of FGM porous shells is conducted. Several parameters including elastic foundation, material distribution, porosity and shell geometry are inspected on their effects to the fundamental frequency of the shell structure. Lastly, a range of parametric studies are conducted for the damping forced vibration analysis of functionally graded porous shells. While the parameters considered in the parametric study regarding the free vibration of FGM porous shells are inspected in this example, additional parameter of damping ratio is also implemented by using Kelvin's viscoelastic model.

Non-dimensional parameters of the elastic foundation which are used in all examples are given as

$$\begin{aligned} k_0 &= \frac{K_0\, D_0}{a^4} \\ k_1 &= \frac{K_1\, D_0}{a^2} \\ D_0 &= \frac{E_m\, h^3}{12\,(1-\upsilon_m^2)} \end{aligned} \tag{27}$$

Table 2 Fundamental frequencies for FGM shells resting on elastic foundation $\left(\bar{\omega} = \omega \frac{a^2}{h}\sqrt{\frac{\rho_c}{E_c}}\right)$

K_0, K_1	$R_x/a\,, R_y/b$	Method	$pl=0$	$pl=0.5$	$pl=1$	$pl=2$	$pl=5$	$pl=10$	$pl=\infty$
(0,0)	*(5,5) Spherical*	Kiani *et al.* (2012a)	6.0767	5.1783	4.6779	4.2397	3.9593	3.8057	3.0901
		Present study	6.0915	5.1999	4.6997	4.2575	3.9623	3.8054	3.1005
	(5,∞) Cylindrical	Kiani *et al.* (2012a)	5.8337	4.9551	4.4692	4.0554	3.8152	3.6803	2.9665
		Present study	5.8460	4.9715	4.4846	4.0658	3.8105	3.6736	2.9755
	(∞,∞) Plate	Kiani *et al.* (2012a)	5.7693	4.8985	4.4175	4.0120	3.7853	3.6550	2.9338
		Present study	5.7697	4.9016	4.4194	4.0089	3.7673	3.6365	2.9367
(100,10)	*(5,5) Spherical*	Kiani *et al.* (2012a)	6.4694	5.6787	5.254	4.9007	4.7003	4.5940	4.0577
		Present study	6.4833	5.6986	5.2738	4.9168	4.7041	4.5953	4.0671
	(5,∞) Cylindrical	Kiani *et al.* (2012a)	6.2419	5.4768	5.0704	4.7442	4.5820	4.4928	3.9646
		Present study	6.2533	5.4919	5.0845	4.7539	4.5794	4.4889	3.9730
	(∞,∞) Plate	Kiani *et al.* (2012a)	6.1829	5.4278	5.0279	4.7111	4.5616	4.4764	3.9430
		Present study	6.1833	5.4308	5.0300	4.7092	4.5480	4.4628	3.9467
(500,50)	*(5,5) Spherical*	Tran *et al.* (2021)	7.8460	7.3475	7.1049	6.9378	6.8999	6.8873	6.6426
		Kiani *et al.* (2012a)	7.8460	7.3468	7.1054	6.9410	6.9097	6.8976	6.6423
		Present study	7.8575	7.3629	7.1212	6.9543	6.9158	6.9024	6.6519
	(5,∞) Cylindrical	Tran *et al.* (2021)	7.6616	7.1964	6.9754	6.8348	6.8270	6.8264	6.5866
		Kiani *et al.* (2012a)	7.6598	7.1943	6.9747	6.8371	6.8363	6.8359	6.5857
		Present study	7.6693	7.2066	6.9863	6.8460	6.8383	6.8376	6.5949
	(∞,∞) Plate	Tran *et al.* (2021)	7.6163	7.1652	6.9528	6.8224	6.8253	6.8272	6.5812
		Kiani *et al.* (2012a)	7.6160	7.1640	6.9527	6.8253	6.8353	6.8374	6.5806
		Present study	7.6163	7.1670	6.9559	6.8261	6.8298	6.8325	6.5868

Table 1 Material features used in study

Material	Properties		
	$\rho\ (kg/m^3)$	$E(GPa)$	ν
Alumina (Al_2O_3)	3800	380	0.3
Aluminium (Al)	2702	70	0.3

Free vibration analysis for FGM porous shell resting on elastic foundation is performed for 3 different geometries (spherical, cylindrical and plate). Subsequently, damped forced vibration analyses are conducted for FGM porous shell supported by elastic foundation and the impact of different geometries, porous coefficients, elastic foundation parameters, damping coefficients and material distribution ratio on the results is investigated. The material properties utilizing in the analysis are as shown in the table.

3.1 Free vibration analysis of FGM shell resting on elastic foundation

In the first part of the performed free vibration analysis, fundamental frequencies the FGM shell supported by elastic foundation is investigated. The boundaries of shell structures are considered to be simply supported on all sides. The geometric properties of the considered shell are $a = b = 1\,m$ and $h = 0.1\,m$. In this example, the parameters affecting the analysis are inspected with various values which are power law coefficients ($pl = 0, 0.5, 1, 2, 5, 10, \infty$) , ratio of the principal radii of curvatures to length and width ($\frac{R_x}{a}, \frac{R_y}{b} = \{5,5\}, \{5, \infty\}, \{\infty, \infty\}$) , elastic foundation parameters ($K_0, K_1 = \{0,0\}, \{100,10\}, \{500,50\}$). Obtained results are compared with the ones available in the literature and given in tabular form.

The fundamental frequencies regarding FGM shells resting on elastic foundation are investigated by Tran et al. (2021) and Kiani *et al.* (2012a) In order to verify the consistency of the obtained results via the developed algorithm, this problem is also investigated in this paper. As can be seen from Table 2, the results available in the literature are very agreeable with the ones presented by this study. It can be understood that the material and elastic foundation parameters are successfully integrated into the developed algorithm.

3.2 Free vibration analysis of FGM porous shell resting on elastic foundation

In this example, free vibration behaviour of simply supported FGM porous shells resting on elastic foundation is investigated via a parametric study. The geometric properties of the shell employed in this example are $a = b = 1\,m$ and $h = 0.1\,m$. The non-dimensional parameters given in Eq. (27) are used also for this example. The parameters inspected in the analysis are power law coefficients ($p_l = 0, 0.5, 1, 2, 5, 10$), geometries (spherical ($R_x = R_y = 5$), cylindrical ($R_x = 5, R_y = \infty$), plate ($R_x = \infty, R_y = \infty$) , porosity coefficients ($p_r = 0, 0.1, 0.2$) and

Table 3 Fundamental frequencies for FGM porous shells resting on elastic foundation $\left(\bar{\omega} = \omega \frac{a^2}{h}\sqrt{\frac{\rho_c}{E_c}}\right)$

K_0, K_1	p_l	Spherical ($R_x = R_y = 5$)			Cylindrical ($R_x = 5,\ R_y = \infty$)			Plate ($R_x = \infty,\ R_y = \infty$)		
		$p_r = 0$	$p_r = 0.1$	$p_r = 0.2$	$p_r = 0$	$p_r = 0.1$	$p_r = 0.2$	$p_r = 0$	$p_r = 0.1$	$p_r = 0.2$
0,0	0	6.0969	6.1337	6.1970	5.8460	5.8824	5.9394	5.7697	5.8041	5.8590
	0.5	5.1999	5.1595	5.1201	4.9715	4.9256	4.8798	4.9016	4.8537	4.8057
	1	4.6997	4.5768	4.4213	4.4846	4.3556	4.1919	4.4194	4.2881	4.1213
	2	4.2575	4.0247	3.6866	4.0658	3.8272	3.4779	4.0089	3.7679	3.4140
	5	3.9623	3.6494	3.1318	3.8105	3.4986	2.9766	3.7673	3.4556	2.9312
	10	3.8054	3.4911	2.9615	3.6736	3.3669	2.8446	3.6365	3.3324	2.81234
100,10	0	6.4833	6.5583	6.6594	6.2533	6.3240	6.4205	6.1833	6.2525	6.3475
	0.5	5.6986	5.7117	5.7374	5.4919	5.5022	5.5251	5.4308	5.4404	5.4624
	1	5.2738	5.2254	5.1667	5.0845	5.0344	4.9738	5.0300	4.9796	4.9184
	2	4.9168	4.7909	4.6080	4.7539	4.6289	4.4463	4.7092	4.5847	4.4024
	5	4.7041	4.5322	4.2466	4.5794	4.4151	4.1386	4.5480	4.3868	4.1141
	10	4.5953	4.4355	4.1632	4.4889	4.3415	4.0859	4.4628	4.3203	4.0717
500,50	0	7.8575	8.0351	8.2539	7.6693	7.8454	8.0625	7.6163	7.79211	8.0090
	0.5	7.3629	7.5253	7.7281	7.2066	7.3703	7.5747	7.1670	7.3317	7.5373
	1	7.1212	7.2616	7.4345	6.9863	7.1300	7.3072	6.9556	7.1013	7.2809
	2	6.9543	7.0681	7.1962	6.8460	6.9664	7.1026	6.8261	6.9500	7.0907
	5	6.9158	7.0292	7.1335	6.8383	6.9628	7.0818	6.8298	6.9603	7.0878
	10	6.9024	7.0418	7.1768	6.8376	6.9905	7.1439	6.8325	6.9926	7.1573

elastic foundation parameters $(K_0, K_1 = \{0,0\}, \{100,10\}, \{500,50\})$.

Table 3 presents the variation in dimensionless fundamental frequencies of functionally graded shell supported by elastic foundation. The analysis considers various shell geometries, power law coefficients, and elastic foundation parameters. The power law coefficient influences the transition rate of material of FG shell from ceramic to metal. As the power law coefficient increases, the transition from ceramic to metal occurs more rapidly. It is known that Young's modulus of metal is lower than that of ceramic. Therefore, an increase in the power law coefficient leads to a reduction in stiffness of FG shell. Consequently, this results in a decrease in the dimensionless fundamental frequencies as the power law coefficients increases. An increase in elastic foundation parameter makes FG shell more rigid. Consequently, as the elastic foundation parameter increases, the dimensionless fundamental frequencies also increase. This increase in dimensionless fundamental frequencies becomes more pronounced at higher power law coefficients. However, in contrast, the most noticeable effect of the power law coefficient is observed when the foundation parameters are at their lowest values. As shell's radius of curvature increases, shell becomes more slender. Therefore, the rigidity of FG shell reduces. As a result, the dimensionless fundamental frequencies of FG shell decrease, as radius of curvature increases. Thus, the relationship between the dimensionless fundamental frequencies for different shell geometries follows the order $\omega_{spherical} > \omega_{cylindrical} > \omega_{plate}$. To examine the effect of porosity coefficient on the dimensionless fundamental frequencies of FG porous sell resting on elastic foundation in more detail, various graphs are generated. Young's modulus and mass density of FG porous shell vary according to thickness, porosity, and power law coefficients. The variation in the average Young's modulus across the thickness of FG porous shell with respect to power law and porosity coefficients is shown in Figs. 3(a), while Fig. 3(b) presents the variation in the average mass density across the thickness with respect to porosity and power law coefficients. Fig. 3(c) and 3(d) illustrate the percentage change in the average Young's modulus and mass density, from $pr = 0$ to $pr = 0.1$ and from $pr = 0.1$ to $pr = 0.2$, according to power law coefficient.

In Table 3, it is observed that when the material is rich in ceramic content ($pl = 0$), the dimensionless fundamental frequencies increase with an increase in the porosity coefficient, contrary to expectations. This is because, a decrease in Young's modulus leads to a reduce in the dimensionless fundamental frequencies, while a decrease in mass density results in an increase in the dimensionless fundamental frequencies and as can be seen from Figs. 3(c) and 3(d), up to a certain value of the power law coefficient, changes in porosity coefficient affect the mass density more significantly than Young's modulus. As the elastic foundation parameters (K_0, K_1) increase, it is observed that the influence of porosity coefficient on increasing the dimensionless fundamental frequencies becomes evident at higher values of the power law coefficient. This can be explained: As the elastic foundation parameters increase, the stiffness of the FG porous shell increases. The effect of the elastic foundation parameters becomes more dominant than the reduction in Young's modulus caused by the

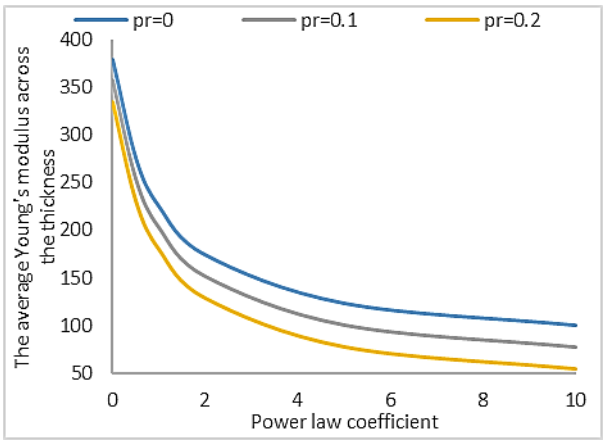

(a)

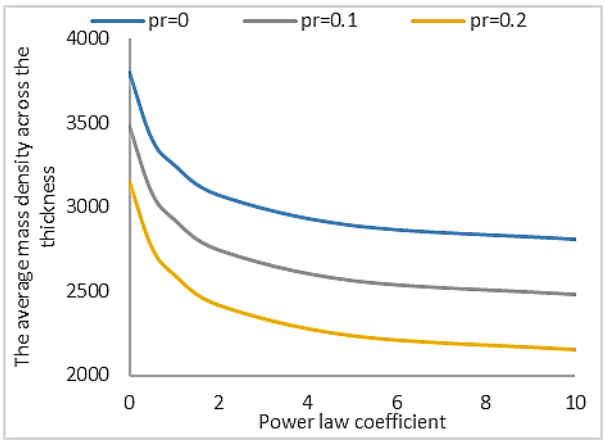

(b)

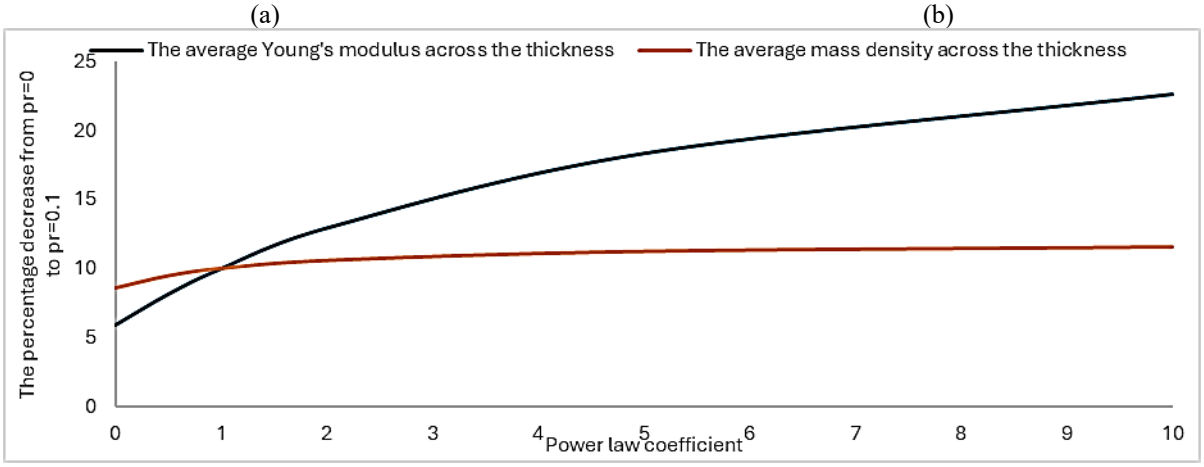

(c)

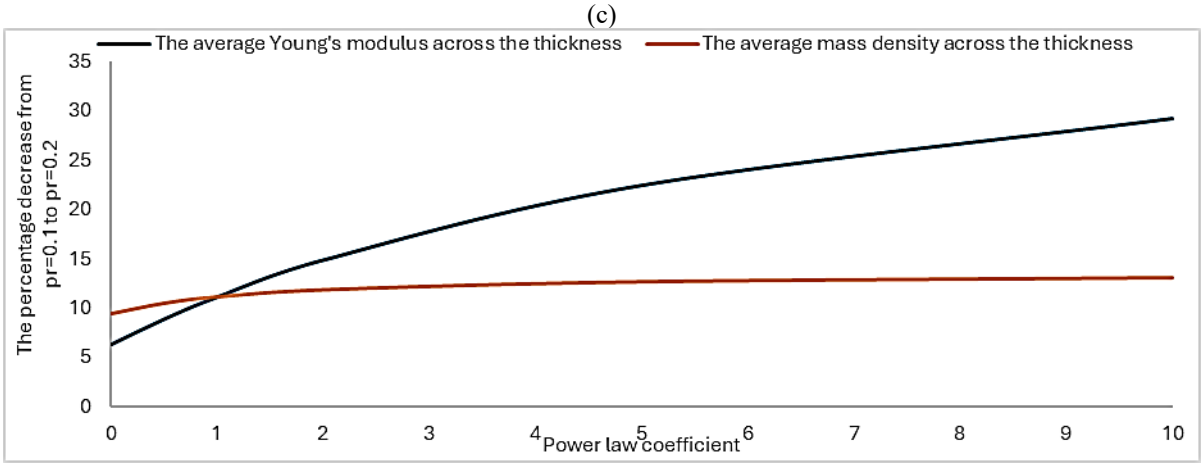

(d)

Fig. 3 The variation in the average Young's modulus and mass density across the thickness with respect to porosity and power law coefficient

increase in porosity, leading to an increase in the dimensionless fundamental frequencies.

3.3 Forced vibration analysis of FGM porous shell resting on elastic foundation

A damped forced vibration analysis is conducted for simply supported FGM porous shell supported by elastic foundation. The non-dimensional parameters used in the damped forced vibration analysis are presented in Eq. (27). Three geometric shapes are chosen to be inspected which are spherical $(R_x = R_y = 5)$, cylindrical $(R_x = 5, R_y = \infty)$ and plate $(R_x = R_y = \infty)$ geometry. The geometric properties of the considered FGM porous shell supported by elastic foundation are $a = b = 1\,m$ and $h = 0.1\,m$. The effects of geometrical shape, power law coefficient, porosity, elastic foundation and damping are observed through graphical collocation. The material properties presented in Table 1 also employed for the forced vibration example. A uniformly distributed impulsive step load with a

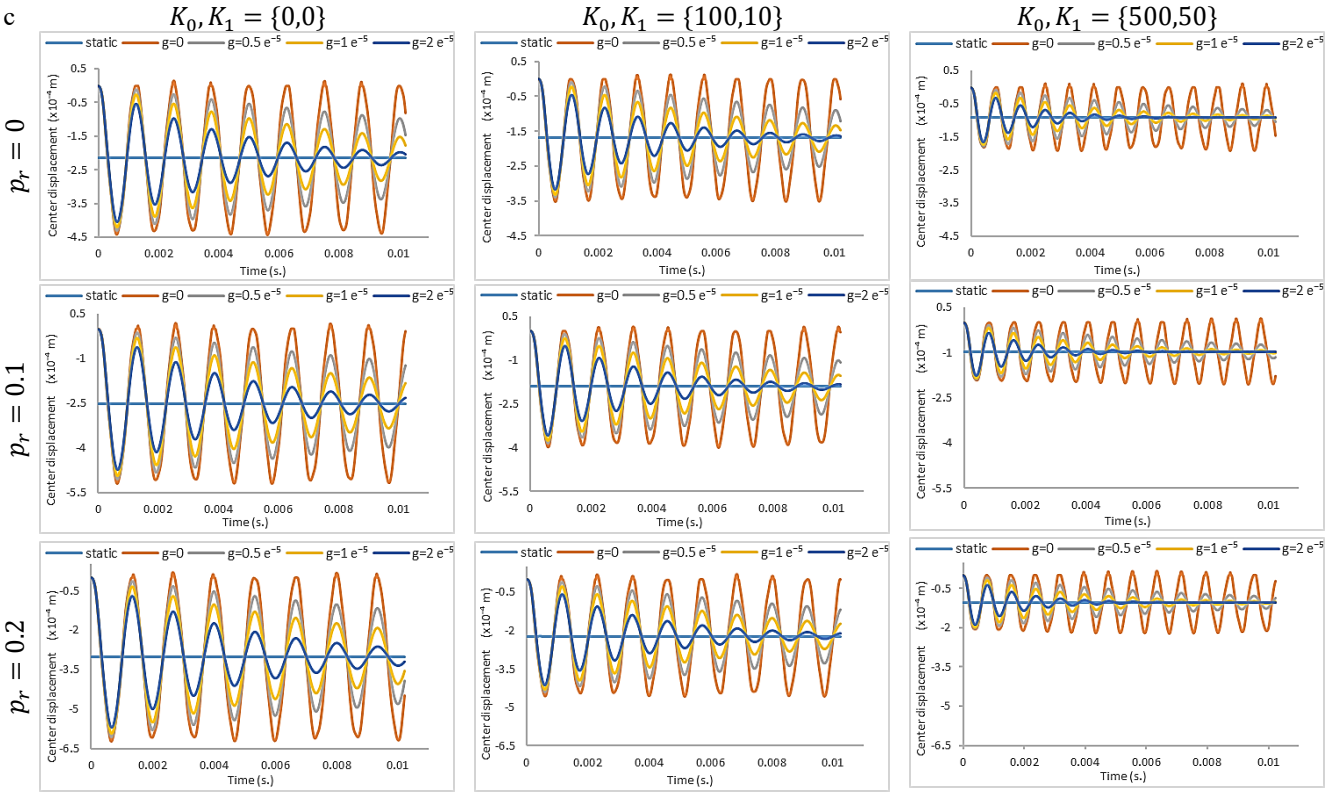

Fig. 4 Displacement at the center point of spherical shell ($p_l = 1$)

magnitude of $q_0 = 10^6\ \mathrm{N}/m^2$ is applied on FGM porous shell. Total analysis duration is $0.01024\ s$ where total number of Laplace parameters is 512. Consequently, time step is $\Delta_t = 2\ e^{-5}\ s$.

The results are given in two styles. In first part general displacement graphics regarding the spherical and cylindrical shell geometries are given in matrix form and the interpretation of yielded results are given referencing their respective figures. Subsequently, comparison studies considering the impact of various parameters on other parameters effects are conducted and their discussions are given in detail with respect to the related figure.

The displacement graphics for spherical and cylindrical shells are given in Figs. 4 and 5, respectively. The displacements vary according to different porosity coefficients, foundation parameters, damping ratios, and shell geometries. In the analyses, the power law coefficient is considered constant. The displacements under investigation are the central displacement for each coefficient and geometry. Interpretation of obtained results given in Figs. 4 and 5 are presented as follows.

Figs. 4 and 5 examine the impact of porosity on the displacement-time relationship. Porosity refers to the voids within the material. Therefore, as porosity increases, a decrease in material strength is expected. Consequently, an increase in porosity coefficient leads to higher displacements. Additionally, due to the same reason, the periods of displacement also elongate. The influence of higher porosity coefficient on displacements becomes more pronounced. Furthermore, it is seen that the influence of porosity on displacement becomes more significant with higher values of the porosity coefficient.

As the elastic foundation parameters increase, the system becomes stiffer, leading to a reduction in displacement magnitudes. The amount of reduction in displacements caused by the increase in parameters of the elastic foundation is higher in cylindrical shells in comparison to spherical shells. Additional stiffness due to elastic foundation decreases the periods of the displacements. Furthermore, increased foundation parameters decline the increasing effect on the displacements of the porosity coefficient.

Damping effect is implemented into the shell structures via Kelvin's viscoelastic model. Damping ratio is well-known to reduce the displacement amplitudes eventually reaching the static case. As expected, while the damping ratio is increasing, the dissipation of the displacements accelerates. Moreover, the effect of damping ratio is further enhanced by the increased foundation parameters. Also, a minimal decrease to the effect of damping can be observed while the porosity coefficient increases. Finally, no significant variation to the periods of oscillations is viewed.

For the simply supported FGM cylindrical $(R_x = 5,\ R_y = \infty)$ shell supported by elastic foundation with the same geometric and material properties, the forced vibration analysis is performed with constant damping ratio ($g = 0$). The variation of the maximum displacement value obtained from the analysis with various values of porosity coefficients ($p_r = 0, 0.1, 0.2$), power law coefficients ($pl = 0, 0.5, 1, 2, 5, 10$) and elastic foundation parameters ($K_0, K_1 = \{0,0\}, \{100,10\}, \{500,50\}$) is observed

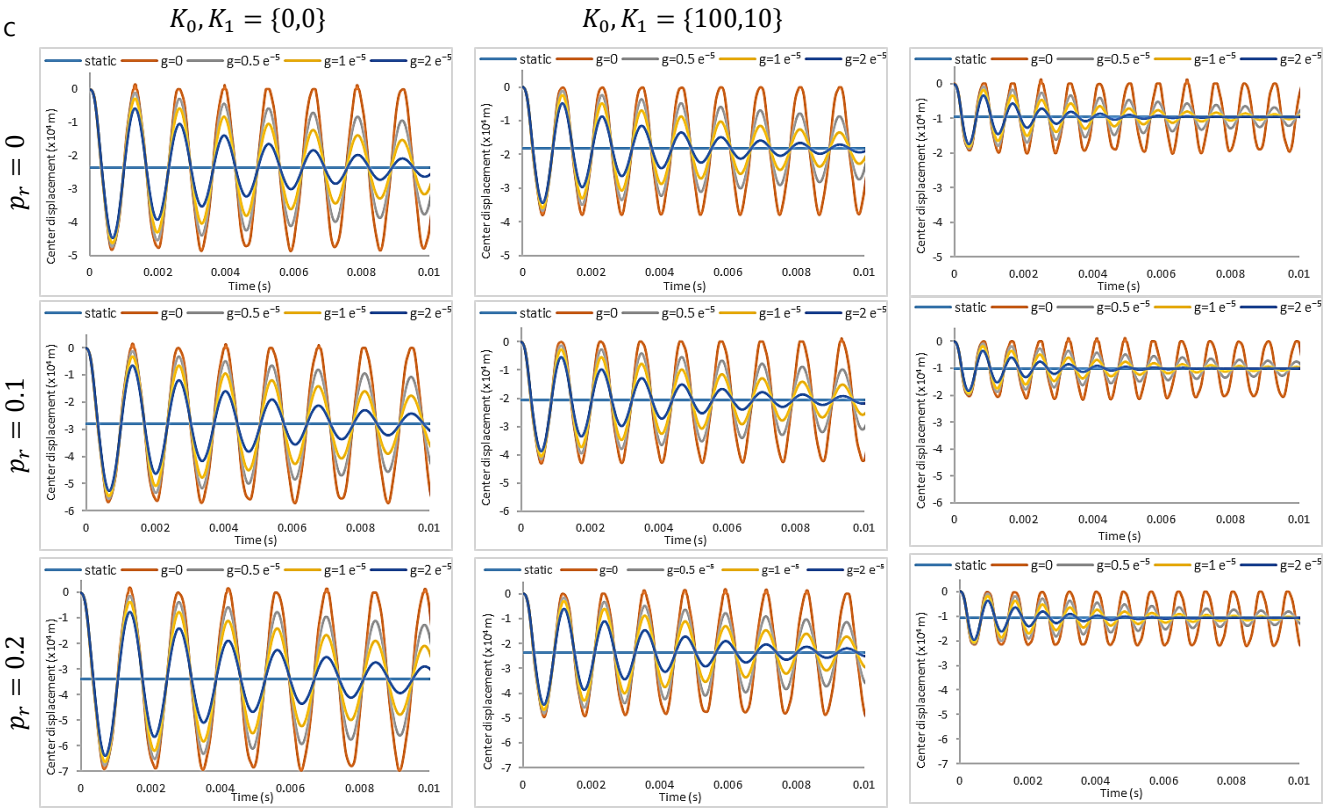

Fig. 5 Displacement at the center point of cylindrical shell ($p_l = 1$)

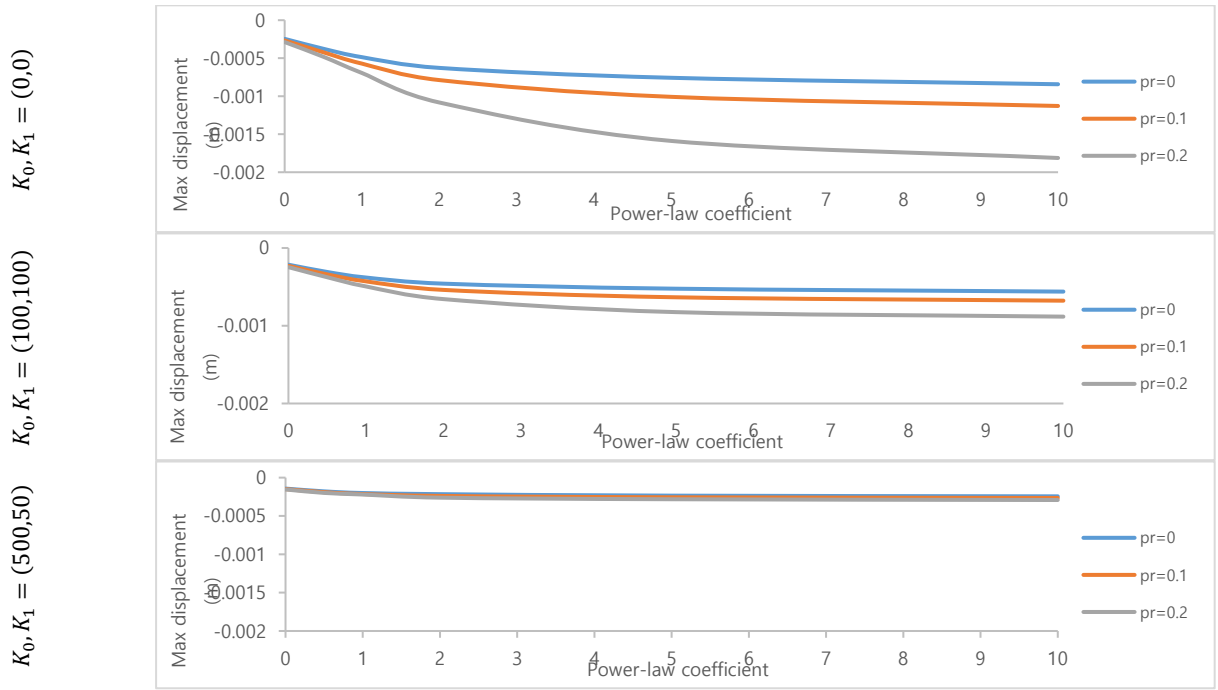

Fig. 6 Maximum displacement at the center point of cylindrical shell

The results obtained from forced vibration analysis of FGM cylindrical porous shell supported by elastic foundation are given in Fig. 6. In this figure, the variation of the maximum displacement values obtained from the forced vibration analysis of FGM porous cylindrical shell with the effect of elastic foundation parameters, porosity coefficient and power law coefficients can be examined. It is observed that the displacements increase with decreasing elastic foundation coefficients for all values of porosity coefficients and power law coefficients. This increase in

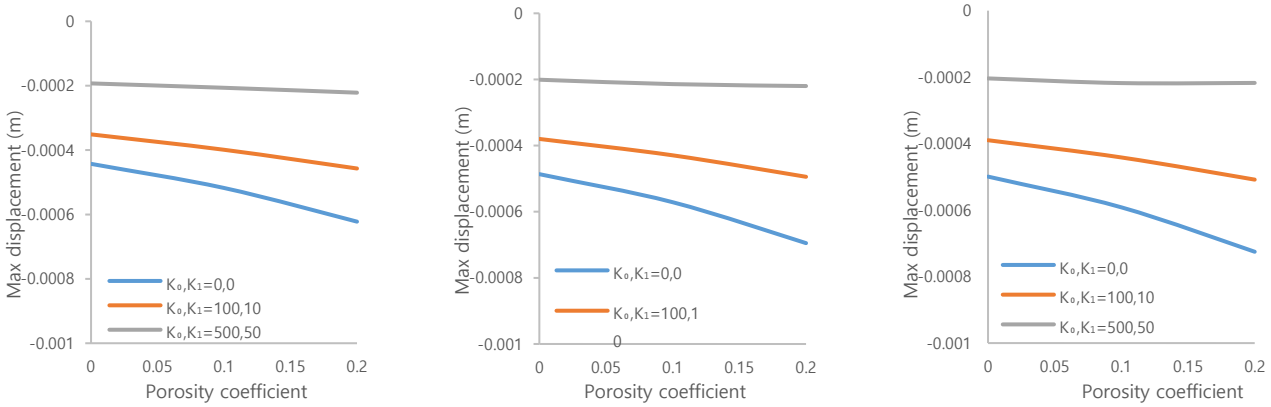

(a) (b) (c)

Fig. 7 Maximum displacement at the center point of (a) spherical shell, (b) cylindrical shell and (c) plate ($g = 0$, $p_l = 1$)

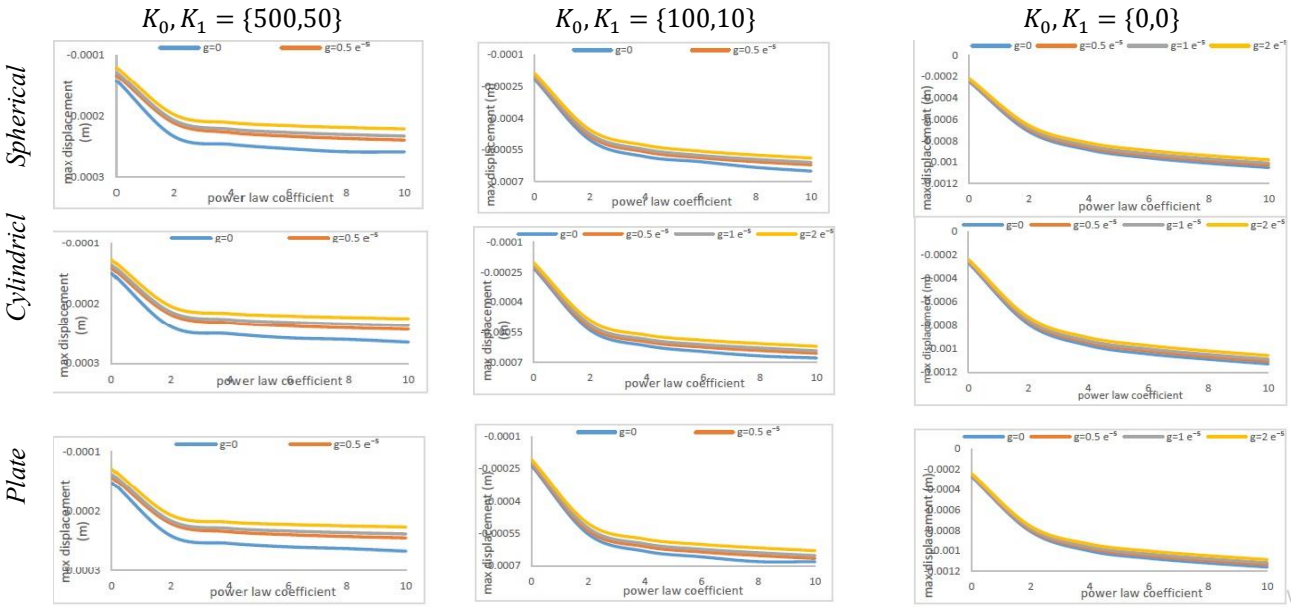

Fig. 8 Maximum displacement at the center point of shell ($p_r = 0.1$)

displacement is attributed to a reduction in the stiffness of FG shell. As shown by the free vibration analysis results, increasing the power law coefficient speeds up the transition of FG shell material from ceramic to metal, making the material richer in metal. Since metal has a lower Young's modulus than ceramic, this transition decreases the stiffness of FG shell. As a result, displacements increase for all porosity coefficients as the power law coefficient rises.

For the same power law coefficient, the difference in displacements for different porosity coefficients initially increase with the power law coefficient. However, this difference tends to stabilize once the power law coefficient reaches a certain value. Additionally, the effect of porosity becomes more pronounced as the porosity coefficient increases, showing a sharp increase in displacements with higher porosity coefficients.

An undamped forced vibration analysis is performed using width, height, length and material properties from the previous analyses. In this part of example, the effects of various geometries (cylindrical ($R_x = 5,\ R_y = \infty$) , spherical ($R_x = 5 = R_y = 5$) and plate ($R_x = \infty,\ R_y = \infty$)) elastic foundation parameters ($K_0, K_1 = (0,0), (100,10), (500,50)$) and porosity coefficients ($p_r = 0, 0.1, 0.2$) on the analysis are investigate.

Fig. 7 contains the results of the forced vibration analysis performed for FGM porous shell supported by elastic foundation. In Fig. 7, the effects of various geometries, porosity coefficients and elastic foundation parameters on the forced vibration analysis are observed. It can be seen that the order of magnitude of the displacements calculated for each value of elastic foundation parameter according to shell geometry is $w_{plate} > w_{cylindrical} > w_{spherical}$. This is because as the curvature radius of FG shell increases, FG shell becomes more slender, which reducing its stiffness. When the

influence of the elastic foundation parameters are investigated, the order of magnitude of displacements according to elastic foundation parameters is $w_{K_0,K_1=(0,0)} > w_{K_0,K_1=(100,10)} > w_{K_0,K_1=(500,50)}$. As expected, displacements increase with the porosity coefficient for all shell geometries. As observed in previous examples, the influence of the porosity coefficient on displacements becomes more pronounced as the porosity coefficient increases

Fig. 8 shows the combined influences of geometry, material distribution, damping, and elastic foundation parameters.

After examining the figure, it can be seen that damping effect is reduced as elastic foundation coefficients get smaller. Additionally, it can be observed that the influence of the power law coefficient on displacements is similar across all damping ratios. The key difference lies in the relationship between elastic foundation parameters and power law coefficient. It is observed that as elastic foundation parameters increase, the displacement increase due to the power law coefficient becomes less pronounced.

At the highest elastic foundation parameters, the displacement increase is noticeable up to a certain point to the power law coefficient. However, beyond this point, the increase in displacement becomes less significant. Finally, changes in shell geometry do not seem to have a significant effect on damping.

4. Conclusions

In this paper, free and damped forced vibration analysis of FGM shells with porosities supported by elastic foundation are investigated. The displacement fields of the examined problems are derived by using HSDT. The equations of motion are derived in Laplace domain via Hamilton's principle. The solution is then achieved by applying Navier's method. An algorithm is developed in Mathematica for this purpose. The yielded results from the parametric studies may be summarized in a few points.

- Elastic foundation parameters have significant influence on the displacements, dimensionless fundamental frequencies and periods. As the elastic foundation parameters increase, FG shell becomes more rigid. Consequently, an increase in the elastic foundation parameter reduces both displacements and periods, while dimensionless fundamental frequencies increase. Moreover, elastic foundation parameters affect the impact of other parameters examined in this study. Specifically, an increase in the elastic foundation parameters diminishes the effects of both the power law and porosity coefficients. The impact of elastic foundation parameters is also consistent across all shell geometries.
- The power law coefficient controls the material distribution throughout the thickness of the shell. As it increases, the transition of the material from ceramic to metal accelerate, implying the elasticity modulus to reduce faster. As expected, reduced elasticity modulus yields greater displacement amplitudes and periods and decrease the dimensionless fundamental frequencies. Additionally, as the power law coefficient increases, its effect on the analyses becomes more pronounced. The obtained results verify these expectations.
- Porosity of the material is implemented into the problems by considering even distribution indicates the volume of voids in material composition. As the porosity coefficient increases, the material strength reduces yielding greater displacement amplitudes and periods. Additionally, the porosity coefficient is affected by all other parameters considered. However, the porosity coefficient does not have a significant impact on damping. An increase in elastic foundation parameters reduces the effect of the porosity coefficient because FG shell becomes more rigid. Moreover, the highest displacement and period are achieved at the maximum power law and porosity coefficients as increases in both coefficients reduce rigidity.
- When examining the impacts of porosity on free vibration analysis, the following conclusions can be drawn. As expected, an increase in porosity increases the void ratio in the material, reduces Young's modulus, and thereby decreases the dimensionless fundamental frequencies. However, the increase in the porosity coefficient also reduces the mass density, which leads to an increase in the dimensionless fundamental frequencies. Up to a certain value of the power law coefficient, changes in porosity coefficient affect the mass density more significantly than Young's modulus. Therefore, up to this specific value of the power law coefficient, an increase in porosity coefficient the dimensionless fundamental frequencies. Beyond this value, increases in porosity lead to a decrease in the dimensionless fundamental frequencies.
- Viscoelasticity models the internal friction of the material. Therefore, as the viscoelasticity parameter (damping ratio) increases the displacements tend to dissipate. For greater values of the damping ratio, the dissipation of the oscillations accelerates. Elastic foundation parameters seem to increase the effect of damping ratio as they increase. In contrast, neither the porosity coefficient nor the power-law coefficient has a significant impact on damping.

References

Ahmadi, H. (2019), "Nonlinear primary resonance of imperfect spiral stiffened functionally graded cylindrical shells surrounded by damping and nonlinear elastic foundation", *Eng. with Comput.*, **35**(4), 1491-1505. https://doi.org/10.1007/s00366-018-0679-2.

Ahmadi, H., Bayat, A. and Duc, N.D. (2021), "Nonlinear forced vibrations analysis of imperfect stiffened fg doubly curved shallow shell in thermal environment using multiple scales method", *Compos. Struct.*, **256**, 113090. https://doi.org/10.1016/j.compstruct.2020.113090.

Ahmadi, H. and Foroutan, K. (2019), "Nonlinear vibration of stiffened multilayer fg cylindrical shells with spiral stiffeners rested on damping and elastic foundation in thermal environment", *Thin-Wall. Struct.*, **145**, 106388. https://doi.org/10.1016/j.tws.2019.106388.

Ahmadi, H. and Foroutan, K. (2020), "Nonlinear static and dynamic thermal buckling analysis of imperfect multilayer fg cylindrical shells with an fg porous core resting on nonlinear

elastic foundation", *J. Therm. Stresses*, **43**(5), 629-649. https://doi.org/10.1080/01495739.2020.1727802.

Al-Toki, M.H.Z., Ali, H.A.K, Faleh, N.M. and Fenjan, R.M. (2022), "Numerical assessment of nonlocal dynamic stability of graded porous beams in thermal environment rested on elastic foundation", *Geomech. Eng*., **28**(5), 455-461. https://doi.org/10.12989/gae.2022.28.5.455.

Alimoradzadeh, M. and Akbas, S.D. (2023), "Nonlinear vibration analysis of carbon nanotube-reinforced composite beams resting on nonlinear viscoelastic foundation", *Geomech. Eng*., **32**(2), 125-135. https://doi.org/10.12989/gae.2023.32.2.125.

Alnujaie, A., Akbas, S.D., Eltaher, M.A. and Assie, A. (2021), "Forced vibration of a functionally graded porous beam resting on viscoelastic foundation", *Geomech. Eng.*, **24**(1), 91-103. https://doi.org/10.12989/gae.2021.24.1.091.

Amiri, M., Loghman, A. and Arefi, M. (2022), "Thermoelastic analysis of rectangular plates with variable thickness made of FGM based on tsdt using DQ method", *Geomech. Eng*., **29**(6), 667-681. https://doi.org/10.12989/gae.2022.29.6.667.

Anh, V.T.T., Huong, V.T., Nguyen, P.D. and Duc, N.D. (2021), "Nonlinear dynamic analysis of porous graphene platelet-reinforced composite sandwich shallow spherical shells", *Mech. Compos, Mater*., **57**(5), 609-622. https://doi.org/10.1007/s11029-021-09983-w.

Avcar, M., Hadji, L. and Akan, R. (2022), "The influence of winkler-pasternak elastic foundations on the natural frequencies of imperfect functionally graded sandwich beams", *Geomech. Eng.*, **31**(1), 99-112. https://doi.org/10.12989/gae.2022.31.1.099.

Barati, M.R. and Zenkour, A.M. (2019), "Vibration analysis of functionally graded graphene platelet reinforced cylindrical shells with different porosity distributions", *Mech. Adv. Mater. Struct.*, **26**(18), 1580-1588. https://doi.org/10.1080/15376494.2018.1444235.

Bayat, M., Bayat, M., Kia, M., Ahmadi, H.R. and Pakar, I. (2018), "Nonlinear frequency analysis of beams resting on elastic foundation using max-min approach", *Geomech. Eng.*, **16**(4), 355-361. https://doi.org/10.12989/gae.2018.16.4.355.

Benaberrahmane, I., Bentoucef, S., Sekkal, M., Mekerbi, M., Bouiadjra, R.B., Selim, M.M., Tounsi, A. and Hussain, M. (2021), "Investigating of free vibration behavior of bidirectional fg beams resting on variable elastic foundation", *Geomech. Eng*., **25**(5), 383-394. https://doi.org/10.12989/gae.2021.25.5.383.

Bennedjadi, M., Aldosari, S.M., Chikh, A., Kaci, A., Bousahla, A.A., Bourada, F., Tounsi, A., Benrahou, K.H. and Tounsi, A. (2023), "Visco-elastic foundation effect on buckling response of exponentially graded sandwich plates under various boundary conditions", *Geomech. Eng*., **32**(2), 159–77. https://doi.org/10.12989/gae.2023.32.2.159.

Calim, F.F. (2003), "Dynamic analysis of viscoelastic, anisotropic curved spatial rod systems", Ph. D. Dissertation; Cukurova University, Adana, Turkey (In Turkish)

Calim, F.F. (2016), "Dynamic response of curved Timoshenko beams resting on viscoelastic foundation", *Struct. Eng. Mech.*, **59**(4), 761-774. https://doi.org/10.12989/sem.2016.59.4.761.

Calim, F.F. and Cuma, Y.C. (2022), "Vibration analysis of nonuniform hyperboloidal and barrel helices made of functionally graded material", *Mech. Based Des. Struct. Mach.*, **50**(11), 3781-3795. https://doi.org/10.1080/15397734.2020.1822181.

Calim, F.F. and Cuma, Y.C. (2023), "Forced vibration analysis of viscoelastic helical rods with varying cross-section and functionally graded material", *Mech. Based Des. Struct. Mach.*, **51**(7), 3620-3631. https://doi.org/10.1080/15397734.2021.1931307.

Cheng, Y., Fu, L., Hou, W., Carcione, J.M., Deng, W. and Wang, Z. (2024), "Thermo-poroelastic AVO modeling of Olkaria geothermal reservoirs", *Geoenergy Sci. Eng.*, **241**, 213166. https://doi.org/10.1016/j.geoen.2024.213166.

Chikr, S.C., Kaci, A., Bousahla, A.A., Bourada, F., Tounsi, A., Bedia, E.A.A., Mahmoud, S.R., Benrahou, K.H. and Tounsi, A. (2020), "A novel four-unknown integral model for buckling response of fg sandwich plates resting on elastic foundations under various boundary conditions using Galerkin's approach", *Geomech. Eng.*, **21**(5), 471-487. https://doi.org/10.12989/gae.2020.21.5.471.

Cuma, Y.C. and Calim, F.F. (2021), "Transient response of functionally graded non-uniform cylindrical helical rods", *Steel Compos. Struct.*, **40**(4), 571-580. https://doi.org/10.12989/scs.2021.40.4.571.

Cuma, Y.C. and Calim, F.F. (2022), "Dynamic response of viscoelastic functionally graded barrel and hyperboloidal coil springs with variable cross-sectional area", *Mech. Time-Dependent Mater.*, **26**(4), 923-937. https://doi.org/10.1007/s11043-021-09520-1.

Cuong-Le, T., Nguyen, K.D., Nguyen-Trong, N., Khatir, S., Nguyen-Xuan, H. and Abdel-Wahab, M. (2021), "A three-dimensional solution for free vibration and buckling of annular plate, conical, cylinder and cylindrical shell of fg porous-cellular materials using IGA", *Compos. Struct.*, **259**, 113216. https://doi.org/10.1016/j.compstruct.2020.113216.

Dang, X.H., Nguyen, V.L., Tran, M.T. and Nguyen Thi, B.P. (2022), "Free vibration characteristics of rotating functionally graded porous circular cylindrical shells with different boundary conditions", *Iranian J. Sci. Technol. T. Mech. Eng*., **46**(1), 167-183. https://doi.org/10.1007/s40997-020-00413-1.

Duc, N.D. and Quan, T.Q. (2014), "Transient responses of functionally graded double curved shallow shells with temperature-dependent material properties in thermal environment", *Eur. J. Mech. - A/Solids* **47**, 101-123. https://doi.org/10.1016/j.euromechsol.2014.03.002.

Eratli, N., Argeso, H., Calim, F.F., Temel, B. and Omurtag, M.H. (2014), "Dynamic analysis of linear viscoelastic cylindrical and conical helicoidal rods using the mixed FEM", *J. Sound Vib*., **333**(16), 3671-3690. https://doi.org/10.1016/j.jsv.2014.03.017.

Faleh, N.M., Fenjan, R.M. and Ahmed, R.A. (2020), "Forced vibrations of multi-phase crystalline porous shells based on strain gradient elasticity and pulse load effects", *J. Vib. Eng. Technol.*, **8**(6), 925-933. https://doi.org/10.1007/s42417-020-00203-8.

Foroutan, K. and Ahmadi, H. (2020), "Nonlinear static and dynamic buckling analyses of imperfect fgp cylindrical shells resting on nonlinear elastic foundation under axial compression", *Int. J. Struct. Stab. Dynam.,* **20**(07), 2050074. https://doi.org/10.1142/S0219455420500741.

Fu, T., Wu, X., Xiao, Z., Chen, Z. and Li, B. (2021a), "Analysis of vibration characteristics of fgm sandwich joined conical–conical shells surrounded by elastic foundations." *Thin-Walled Struct.*, **165**, 107979. https://doi.org/10.1016/j.tws.2021.107979.

Fu, T., Wu, X., Xiao, Z. and Chen, Z. (2020), "Thermoacoustic response of porous FGM cylindrical shell surround by elastic foundation subjected to nonlinear thermal loading", *Thin-Walled Struct*., **156**, 106996. https://doi.org/10.1016/j.tws.2020.106996.

Fu, T., Wu, X., Xiao, Z. and Chen, Z. (2021b), "Dynamic instability analysis of porous FGM conical shells subjected to parametric excitation in thermal environment within FSDT", *Thin-Wall. Struct*., **158**, 107202. https://doi.org/10.1016/j.tws.2020.107202.

Ghasemi, A.R. and Meskini, M. (2019), "Free vibration analysis of porous laminated rotating circular cylindrical shells", *J. Vib. Control*, **25**(18), 2494-2508. https://doi.org/10.1177/1077546319858227.

Gao, Q., Ding, Z. and Liao, W. (2022), "Effective elastic

properties of irregular auxetic structures", *Compos. Struct.*, 287, 115269. https://doi.org/10.1016/j.compstruct.2022.115269.

He, Q., Zhou, Y.L., Li, M., He, L. and Dai, H.L. (2023), "Nonlinear vibration analysis of CFRR sandwich doubly-curved shallow shells with a porous microcapsule coating in hygrothermal environment", *Thin-Wall. Struct*., **185**, 110587. https://doi.org/10.1016/j.tws.2023.110587.

Jouneghani, F.Z., Dimitri, R., Bacciocchi, M. and Tornabene, F. (2017), "Free vibration analysis of functionally graded porous doubly-curved shells based on the first-order shear deformation theory", *Appl. Sci*., **7**(12), 1252. https://doi.org/10.3390/app7121252.

Khaniki, H.B. and Ghayesh, M.H. (2023), "Highly nonlinear hyperelastic shells: statics and dynamics", *Int. J. Eng. Sci*., **183**, 103794. https://doi.org/10.1016/j.ijengsci.2022.103794.

Kiani, Y., Akbarzadeh, A.H., Chen, Z.T. and Eslami, M.R. (2012a), "Static and dynamic analysis of an fgm doubly curved panel resting on the pasternak-type elastic foundation", *Compos. Struct*., **94**(8), 2474-2484. https://doi.org/10.1016/j.compstruct.2012.02.028.

Kiani, Y., Shakeri, M. and Eslami, M.R. (2012b), "Thermoelastic free vibration and dynamic behaviour of an FGM doubly curved panel via the analytical hybrid Laplace–Fourier transformation", *Acta Mechanica*, **223**(6) 1199-1218. https://doi.org/10.1007/s00707-012-0629-9.

Kim, Y.W. (2015), "Free vibration analysis of FGM cylindrical shell partially resting on pasternak elastic foundation with an oblique edge", *Compos. Part B: Eng*., **70**, 263-276. https://doi.org/10.1016/j.compositesb.2014.11.024.

Li, H., Hao, Y.X., Zhang, W., Liu, L.T., Yang, S.W. and Wang, D.M. (2021), "Vibration analysis of porous metal foam truncated conical shells with general boundary conditions using GDQ", *Compos. Struct.,* **269**, 114036. https://doi.org/10.1016/j.compstruct.2021.114036.

Li, H., Pang, F., Ren, Y., Miao, X. and Ye, K. (2019a), "Free vibration characteristics of functionally graded porous spherical shell with general boundary conditions by using first-order shear deformation theory", *Thin-Wall. Struct.*, **144**, 106331. https://doi.org/10.1016/j.tws.2019.106331.

Li, H., Pang, F., Chen, H. and Du, Y. (2019b), "Vibration analysis of functionally graded porous cylindrical shell with arbitrary boundary restraints by using a semi analytical method", *Compos. Part B: Eng.,* **164**, 249-264. https://doi.org/10.1016/j.tws.2019.106331.

Liang, X., Zha, X., Yu, Y., Cao, Z., Jiang, X. and Leng, J. (2019), "Semi-Analytical vibration analysis of fgm cylindrical shells surrounded by elastic foundations in a thermal environment", *Compos. Struct*., **223**, 110997. https://doi.org/10.1016/j.compstruct.2019.110997.

Limkatanyu, S., Sae-Long, W., Damrongwiriyanupap, N., Imjai, T., Chaimahawan, P., Sukontasukkul, P., Chompoorat, T. and Hansapinyo, C. (2023), "Nonlinear shear-flexure-interaction rc frame element on winkler-pasternak foundation", *Geomech. Eng*., **32**(1), 69-84. https://doi.org/10.12989/gae.2023.32.1.069.

Liu, K., Zong, S., Li, Y., Wang, Z., Hu, Z. and Wang, Z. (2022), "Structural response of the U-type corrugated core sandwich panel used in ship structures under the lateral quasi-static compression load", *Mar. Struct.*, **84**, 103198. https://doi.org/10.1016/j.marstruc.2022.103198.

Liu, Y., Qin, Z. and Chu, F. (2021), "Nonlinear forced vibrations of fgm sandwich cylindrical shells with porosities on an elastic substrate", *Nonlinear Dynam.,* **104**(2), 1007-1021. https://doi.org/10.1007/s11071-021-06358-7.

Mehala, T., Belabed, Z., Tounsi, A. and Beg, O.A. (2018), "Investigation of influence of homogenization models on stability and dynamic of fgm plates on elastic foundations", *Geomech. Eng*., **16**(3), 257-271. https://doi.org/10.12989/gae.2018.16.3.257.

Melaibari, A., Daikh, A.A., Basha, M., Abdalla, A.W., Othman, R., Almitani, K.H., Hamed,M.A., Abdelrahman, A. and Eltaher, M.A. (2022), "Free vibration of FG-CNTRCs nano-plates/shells with temperature-dependent properties", *Mathematics*, **10**(4), 583. https://doi.org/10.3390/math10040583

Merzoug, M., Bourada, M., Sekkal, M., Abir, A.C., Chahrazed, B., Benyoucef, S. and Benachour, A. (2020), "2D and quasi 3D computational models for thermoelastic bending of fg beams on variable elastic foundation: effect of the micromechanical models", *Geomech. Eng*., **22**(4), 361-374. https://doi.org/10.12989/gae.2020.22.4.361.

Mirjavadi, S.S., Forsat, M., Barati, M.R. and Hamouda, A.M.S. (2022), "Geometrically nonlinear vibration analysis of eccentrically stiffened porous functionally graded annular spherical shell segments", *Mech. Based Des. Struct. Mach.*, **50**(6), 2206-2220. https://doi.org/10.1080/15397734.2020.1771729.

Nebab, M., Benguediab, S., Atmane, H.A. and Bernard, F. (2020), "A simple Quasi-3D HDST for dynamic behavior of advanced composite plates with the effect of variables elastic foundations", *Geomech. Eng.,* **22**(5), 415-431. https://doi.org/10.12989/gae.2020.22.5.415.

Nguyen, V.L., Tran, M.T., Nguyen, V.L. and Le, Q.H. (2021), "Static behaviour of functionally graded plates resting on elastic foundations using neutral surface concept", *Arch. Mech. Eng.*, 5-22. https://doi.org/10.24425/ame.2020.131706.

Pradyumna, S., Nanda, N. and Bandyopadhyay, J.N. (2010), "Geometrically nonlinear transient analysis of functionally graded shell panels using a higher-order finite element formulation", *J. Mech. Eng. Res*., **2**(2) 39-51.

Qin, B., Wang, Q., Zhong, R., Zhao, X. and Shuai, C. (2020), "A three-dimensional solution for free vibration of FGP-GPLRC cylindrical shells resting on elastic foundations: a comparative and parametric study", *Int. J Mech. Sci*., **187**, 105896. https://doi.org/10.1016/j.ijmecsci.2020.105896.

Quan, T.Q. and Duc, N.D. (2016), "Nonlinear vibration and dynamic response of shear deformable imperfect functionally graded double-curved shallow shells resting on elastic foundations in thermal environments", *J. Therm. Stresses*, **39**(4), 437-459. https://doi.org/10.1080/01495739.2016.1158601.

Rabhi, M., Benrahou, K.H., Kaci, A., Houri, M.S.A., Bourada, F., Bousahla, A.A., Tounsi, A., Adda Bedia, E.A., Mahmoud, S.R. and Tounsi, A. (2020), "A new innovative 3-unknowns HSDT for buckling and free vibration of exponentially graded sandwich plates resting on elastic foundations under various boundary conditions", *Geomech. Eng.*, **22**(2), 119-132. https://doi.org/10.12989/gae.2020.22.2.119.

Rachedi, M.A., Benyoucef, S., Bouhadra, A., Bouiadjra, R.B., Sekkal, M. and Benachour, A. (2020), "Impact of the homogenization models on the thermoelastic response of FG plates on variable elastic foundation", *Geomech. Eng.*, **22**(1), 65-80. https://doi.org/10.12989/gae.2020.22.1.065.

Rachid, A., Ouinas, D., Lousdad, A., Zaoui, F.Z., Achour, B., Gasmi, H., Butt, T.A. and Tounsi, A. (2022), "Mechanical behavior and free vibration analysis of fg doubly curved shells on elastic foundation via a new modified displacements field model of 2D and quasi-3D HSDTs", *Thin-Wall. Struct.*, **172**, 108783. https://doi.org/10.1016/j.tws.2021.108783.

Rahimi, A., Alibeigloo, A. and Safarpour, M. (2020), "Three-dimensional static and free vibration analysis of graphene platelet–reinforced porous composite cylindrical shell", *J. Vib. Control*, **26**(19-20), 1627-1645. https://doi.org/10.1177/1077546320902340.

Ramteke, P.M., Kumar, V., Sharma N. and Panda, S.K. (2022), "Geometrical nonlinear numerical frequency prediction of porous functionally graded shell panel under thermal

environment", *Int. J. Nonlinear Mech.,* **143**, 104041. https://doi.org/10.1016/j.ijnonlinmec.2022.104041.

Reddy, J.N. (1984), "Exact solutions of moderately thick laminated shells", *J. Eng. Mech*., **110**(5) 794-809. https://doi.org/10.1061/(ASCE)0733-9399(1984)110:5(794).

Sae-Long, W., Limkatanyu, S., Hansapinyo, C., Prachasaree, W., Rungamornrat, J. and Kwon, M. (2021), "Nonlinear flexibility-based beam element on winkler-pasternak foundation", *Geomech. Eng*., **24**(4), 371-388. https://doi.org/10.12989/gae.2021.24.4.371.

Said, S.M. (2023), "A novel model of a nonlocal porous thermoelastic solid with temperature-dependent properties using an eigenvalue approach", *Geomech. Eng.*, **32**(2), 137-144. https://doi.org/10.12989/gae.2023.32.2.137.

Salehipour, H., Shahgholian-Ghahfarokhi, D., Shahsavar, A., Civalek, O. and Edalati, M. (2020), "Static deflection and free vibration analysis of functionally graded and porous cylindrical micro/nano shells based on the three-dimensional elasticity and modified couple stress theories", *Mech. Based Des. Struct. Mach*., **50**(6), 2184-2205. https://doi.org/10.1080/15397734.2020.1775095.

Sayyad, A.S. and Ghugal, Y.M. (2019), "Static and free vibration analysis of laminated composite and sandwich spherical shells using a generalized higher-order shell theory", *Compos. Struct*., **219**, 129-146. https://doi.org/10.1016/j.compstruct.2019.03.054.

Sayyad, A.S. and Ghugal, Y.M. (2021), "Static and free vibration analysis of doubly-curved functionally graded material shells", *Compos. Struct*., **269**, 114045. https://doi.org/10.1016/j.compstruct.2021.114045.

Sayyad, A.S. and Ghugal, Y.M. (2022), "A unified formulation of various shell theories for the analysis of laminated composite spherical shells", *Vietnam J. Mech*., **44**(2), 97-116. https://doi.org/10.15625/0866-7136/15715.

Sharma, N., Tiwari, P., Maiti, D.K. and Maity, D. (2021), "Free vibration analysis of functionally graded porous plate using 3-D degenerated shell element", *Compos. Part C: Open Access*, ***6***, 100208. https://doi.org/10.1016/j.jcomc.2021.100208.

She, G.L. and. Li, Y.P (2022), "Wave propagation in an FG circular plate in thermal environment", *Geomech. Eng*., **31**(6), 615–22. https://doi.org/10.12989/gae.2022.31.6.615.

Shi, X., Zuo, P., Zhong, R., Guo, C. and Wang, Q. (2022) "Thermal vibration analysis of functionally graded conical-cylindrical coupled shell based on spectro-geometric method." *Thin-Wall. Struct*., **175**, 109138. https://doi.org/10.1016/j.tws.2022.109138.

Sobhani, E., Koohestani, M., Civalek, O. and Avcar, M. (2023), "Natural frequency investigation of graphene oxide powder nanocomposite cylindrical shells surrounded by winkler/pasternak/kerr elastic foundations with a focus on various boundary conditions", *Eng. Anal. Bound. Elem*., **149**, 38-51. https://doi.org/10.1016/j.enganabound.2023.01.012.

Sobhy, M. and Zenkour, A.M. (2019), "Vibration analysis of functionally graded graphene platelet-reinforced composite doubly-curved shallow shells on elastic foundations", *Steel Compos. Struct.*, **33**(2), 195–208. https://doi.org/10.12989/scs.2019.33.2.195.

Sofiyev, A.H. (2010), "The buckling of FGM truncated conical shells subjected to axial compressive load and resting on winkler–pasternak foundations", *Int. J. Pres. Ves. Pip*., **87**(12), 753-761. https://doi.org/10.1016/j.ijpvp.2010.08.012.

Sun, S., Guo, C., Feng, W. and Cao, D. (2022), "Nonlinear vibration analysis of CNT-reinforced functionally graded composite cylindrical shells resting on elastic foundations", *Int. J. Nonlinear Mech*., **143**, 104037. https://doi.org/10.1016/j.ijnonlinmec.2022.104037.

Swaminathan, K., Hirannaiah, S. and Rajanna, T. (2022), "Vibration and stability characteristics of functionally graded sandwich plates with/without porosity subjected to localized edge loadings", *Mech. Based Des. Struct. Mach*., 1-39. https://doi.org/10.1080/15397734.2022.2038619.

Temel, B. and Calim, F.F. (2003), "Forced vibration of cylindrical helical rods subjected to impulsive loads", *J. Appl. Mech.*, **70**(2), 281-291. https://doi.org/10.1115/1.1554413.

Temel, B., Calim, F.F. and Tütüncü, N. (2004), "Quasi-static and dynamic response of viscoelastic helical rods", *J. Sound Vib.*, **271**(3), 921-935. https://doi.org/10.1016/S0022-460X(03)00760-0.

Thai, H.T. and Choi, D.H. (2011), "A refined plate theory for functionally graded plates resting on elastic foundation", *Compos. Sci. Technol*., **71**(16), 1850-1858. https://doi.org/10.1016/j.compscitech.2011.08.016.

Thang, P.T., Do, D.T.T., Nguyen, T.T., Lee, J. and Nguyen-Thoi, T. (2022), "Free vibration characteristic analysis of functionally graded shells with porosity and neutral surface effects", *Ocean Eng*., **255**, 111377. https://doi.org/10.1016/j.oceaneng.2022.111377.

Timesli, A. (2022), "Analytical modeling of buckling behavior of porous FGM cylindrical shell embedded within an elastic foundation", *Gazi Univ. J. Sci*., **35**(1), 148-165. https://doi.org/10.35378/gujs.860783.

Tran, M.T., Nguyen, V.L. and Trinh, A.T. (2017), "Static and vibration analysis of cross-ply laminated composite doubly curved shallow shell panels with stiffeners resting on Winkler–Pasternak elastic foundations", *Int. J. Adv. Struct. Eng*., **9**, 153-164. https://doi.org/10.1007/s40091-017-0155-z

Tran, T.T, Tran, V.K., Pham, Q.H. and Zenkour, A.M. (2021), "Extended four-unknown higher-order shear deformation nonlocal theory for bending, buckling and free vibration of functionally graded porous nanoshell resting on elastic foundation", *Compos. Struct*., **264**, 113737. https://doi.org/10.1016/j.compstruct.2021.113737.

Trinh, M.C. and Kim, S.E. (2019), "A three variable refined shear deformation theory for porous functionally graded doubly curved shell analysis", *Aerosp. Sci. Technol.,* **94**, 105356. https://doi.org/10.1016/j.ast.2019.105356.

Türker, H.T., Cuma, Y.C. and Calim, F.F. (2023), "An efficient approach for free vibration behaviour of non-uniform and non-homogeneous helices", *Iranian J. Sci. Tech. T. Civil Eng*., **47**, 1959-1970. https://doi.org/10.1007/s40996-023-01075-0.

Vinh, V.P. and Tounsi, A. (2022), "Free vibration analysis of functionally graded doubly curved nanoshells using nonlocal first-order shear deformation theory with variable nonlocal parameters", *Thin-Wall. Struct.*, **174**, 109084. https://doi.org/10.1016/j.tws.2022.109084.

Vu, T.V., Cao, H.L., Truong, G.T. and Kim, C.S. (2023), "Buckling analysis of the porous sandwich functionally graded plates resting on Pasternak foundations by Navier solution combined with a new refined quasi-3D hyperbolic shear deformation theory", *Mech. Based Des. Struct. Mach.*, **51**(11), 6227-6253. https://doi.org/10.1080/15397734.2022.2038618.

Wang, J., Wang, Y.Q. and Chai, Q. (2022), "Free vibration analysis of a spinning functionally graded spherical–cylindrical–conical shell with general boundary conditions in a thermal environment", *Thin-Wall. Struct.*, **180**, 109768. https://doi.org/10.1016/j.tws.2022.109768.

Wang, Y., Ye, C. and Zu, J.W. (2018), "Identifying the temperature effect on the vibrations of functionally graded cylindrical shells with porosities", *Appl. Math. Mech.*, **39**(11), 1587-1604. https://doi.org/10.1007/s10483-018-2388-6.

Wang, Y. and Wu, D. (2017), "Free vibration of functionally graded porous cylindrical shell using a sinusoidal shear deformation theory", *Aerosp. Sci. Technol*., **66**, 83-91. https://doi.org/10.1016/j.ast.2017.03.003.

Wu, M., Wang, B., Ba, Z., Dai, K. and Liang, J. (2024),

"Propagation attenuation of elastic waves in multi-row infinitely periodic pile barriers: A closed-form analytical solution", *Eng. Struct.*, **315**, 118480. https://doi.org/10.1016/j.engstruct.2024.118480.

Xiao, H., Yan, K. and She, G. (2021), "Study on the characteristics of wave propagation in functionally graded porous square plates", *Geomech. Eng.*, **26**(6), 607-615. https://doi.org/10.12989/gae.2021.26.6.607.

Younsi, A., Tounsi, A., Zaoui, F.Z. and Bousahla, A.A. (2018), "Novel Quasi-3D and 2D shear deformation theories for bending and free vibration analysis of FGM plates", *Geomech. Eng.*, **14**(6), 519-532. https://doi.org/10.12989/gae.2018.14.6.519.

Zannon, M., Abu-Rqayiq, A. and Al-bdour, A. (2020), "Free vibration frequency of thick FGM spherical shells based on a third-order shear deformation theory", *Eur. J. Pure App., Math.,* **13**(4), 766-778. https://doi.org/10.29020/nybg.ejpam.v13i4.3826.

Zaoui, F.Z., Ouinas, D. and Tounsi, A. (2019), "New 2D and quasi-3D shear deformation theories for free vibration of functionally graded plates on elastic foundations", *Compos. Part B: Eng.*, **159**, 231-247. https://doi.org/10.1016/j.compositesb.2018.09.051.

Zenkour, A.M., Allam, M.N.M., Shaker, M.O. and Radwan, A.F. (2011), "On the simple and mixed first-order theories for plates resting on elastic foundations", *Acta Mechanica***220**(1), 33-46. *Compos* 10.1007/s00707-011-0453-7.

Zhang, C., Jin, Q., Song, Y., Wang, J., Sun, L., Liu, H., Dun, L., Tai, H., Yuan, X., Xiao, H., Zhu, L. and Guo, S. (2021), "Vibration analysis of a sandwich cylindrical shell in hygrothermal environment", *Nanotechnol. Rev.*, **10**(1), 414-430. https://doi.org/10.1515/ntrev-2021-0026.

Zhang, J. and Zhang, C. (2023), "Using viscoelastic materials to mitigate earthquake-induced pounding between adjacent frames with unequal height considering soil-structure interactions", *Soil Dyn. Earthq. Eng.*, **172**, 107988. https://doi.org/10.1016/j.soildyn.2023.107988.

Zhang, S., Liu, L., Zhang, X., Zhou, Y. and Yang, Q. (2024), "Active vibration control for ship pipeline system based on PI-LQR state feedback", *Ocean Eng.*, **310**, 118559. https://doi.org/10.1016/j.oceaneng.2024.118559.

Zhao, J., Xie, F., Wang, A., Shuai, C., Tang, J. and Wang, Q. (2019), "A unified solution for the vibration analysis of functionally graded porous (FGP) shallow shells with general boundary conditions", *Compos. Part B: Eng.*, **156**, 406-424. https://doi.org/10.1016/j.compositesb.2018.08.115.

Zhu, C., Fang, X. and Nie, G. (2021), "Nonlinear free and forced vibration of porous piezoelectric doubly-curved shells based on NUEF model", *Thin-Wall. Struct.*, **163**, 107678. https://doi.org/10.1016/j.tws.2021.107678.

Zouatnia, N., Hadji, L. and Kassoul, A. (2018), "An efficient and simple refined theory for free vibration of functionally graded plates under various boundary conditions", *Geomech. Eng.*, **16**(1), 1-9. https://doi.org/10.12989/gae.2018.16.1.001.

CC